SensCon: Embedding Physiological Sensing into Virtual Reality Controllers

FRANCESCO CHIOSSI, LMU Munich, Germany
THOMAS KOSCH, HU Berlin, Germany
LUCA MENGHINI, University of Trento, Italy
STEEVEN VILLA, LMU Munich, Germany
SVEN MAYER, LMU Munich, Germany

Virtual reality experiences increasingly use physiological data for virtual environment adaptations to evaluate user experience and immersion. Previous research required complex medical-grade equipment to collect physiological data, limiting real-world applicability. To overcome this, we present SensCon for skin conductance and heart rate data acquisition. To identify the optimal sensor location in the controller, we conducted a first study investigating users' controller grasp behavior. In a second study, we evaluated the performance of SensCon against medical-grade devices in six scenarios regarding user experience and signal quality. Users subjectively preferred SensCon in terms of usability and user experience. Moreover, the signal quality evaluation showed satisfactory accuracy across static, dynamic, and cognitive scenarios. Therefore, SensCon reduces the complexity of capturing and adapting the environment via real-time physiological data. By open-sourcing SensCon, we enable researchers and practitioners to adapt their virtual reality environment effortlessly. Finally, we discuss possible use cases for virtual reality-embedded physiological sensing.

CCS Concepts: • **Human-centered computing → Usability testing**.

Additional Key Words and Phrases: Virtual Reality, Controller, Physiological Computing, Physiological Interaction, Embedded Systems, Wearable Computing

ACM Reference Format:
Francesco Chiossi, Thomas Kosch, Luca Menghini, Steeven Villa, and Sven Mayer. 2023. SensCon: Embedding Physiological Sensing into Virtual Reality Controllers. *Proc. ACM Hum.-Comput. Interact.* 7, MHCI, Article 223 (September 2023), 32 pages. https://doi.org/10.1145/3604270

1 INTRODUCTION

Virtual Reality (VR) allows manipulation and control of diverse stimuli in virtual environments as close as possible to real-world ones. Besides the immersion in VR, different responses can be triggered for users, including engagement [51], presence [96], arousal [35], and workload [69]. Evaluating these factors is pivotal in user experience (UX) research in VR. To evaluate such responses, researchers often use post hoc assessments (e.g., questionnaires) since real-time user input is challenging or even hardly possible [106]. Recently, implicit real-time assessments such as physiological measures, have become increasingly popular to overcome these drawbacks. They offer real-time control and quantitative measures of user behavior when exposed to VR and adaptation

Authors' addresses: Francesco Chiossi, LMU Munich, Munich, 80337, Germany, francesco.chiossi@um.ifi.lmu.de; Thomas Kosch, HU Berlin, Berlin, , Germany, thomas.kosch@hu-berlin.de; Luca Menghini, University of Trento, Rovereto, 38068, Italy, luca.menghini-1@unitn.it; Steeven Villa, LMU Munich, Munich, 80337, Germany, steeven.villa@um.ifi.lmu.de; Sven Mayer, LMU Munich, Munich, 80337, Germany, info@sven-mayer.com.

2573-0142/2023/9-ART223 $15.00
https://doi.org/10.1145/3604270

to virtual environments. Peripheral physiological responses, such as Electrodermal Activity (EDA) and photoplethysmography (PPG), are indicative metrics for physiological arousal [107], emotional valence [74], or cognitive workload [45].

Current scientific measurement standards require medical-grade devices, whose signal recording quality comes at the cost of limited ecological validity [53, 88] and unintuitive VR synchronization [112]. Recording physiological data in VR requires ad-hoc preprocessing pipelines to disentangle physiological signals from movement artifacts, increasing demands for technical synchronization and data analysis [46]. To lower the entry hurdle, researchers designed [110] and prototyped [14] physiological sensors embedded into VR systems. For instance, Luong et al. [70] estimated the mental workload in a VR flight simulation in real-time using multiple physiological inputs embedded in the HMD. However, available validation studies are either limited to consumer-grade devices [77] or are not applied to VR environments [105].

In this paper, we present SensCon, a physiological sensing system that incorporates EDA and PPG measurements into VR controllers allowing for mobile and flexible interactions, cf. [1, 2]. In contrast to bulky medical-grade equipment such as depicted in Figure 5, SensCon encompasses an easy and ready-to-use system designed to minimize the user's preparation time. Here, we first ran a study investigating how users hold VR controllers to inform sensor placement. Then we evaluated the SensCon in terms of usability, user experience, and measurement accuracy compared to medical-grade devices across six different VR tasks. We found significant differences concerning usability and user experience favouring SensCon compared to medical-grade equipment. Furthermore, we find that SensCon delivers EDA and PPG data that can be used as a measure for user experience evaluation. Finally, we conclude how large-scale assessments of EDA and PPG can be used to create individually-tailored immersive environments for VR users.

The contribution of this work is fourfold. First, we conducted a study (Study 1) investigating how users hold VR controllers (N=12) and identified grasping locations with the highest contact probability to identify suitable placing options for EDA and PPG sensing. Second, we implemented SensCon, an unobtrusive and ready-to-use physiological data acquisition system embedded into VR controllers sensing EDA and PPG. Third, we present an evaluation of SensCon in a user study (Study 2, N=12) by assessing the measurement agreement between SensCon and medical-grade devices. Finally, we discuss how our findings can be generalized to future physiologically-aware applications that sense user states in real time. Overall, our work contributes to developing physiological sensing in interactive systems, providing insights into designing and implementing unobtrusive sensing systems for VR controllers and evaluating their performance compared to medical-grade devices.

2 RELATED WORK

In the following, we highlight the relevance of employing physiological measures for improving VR usability and designing adaptive systems in VR settings focusing on EDA and PPG measures. Finally, we summarize previous work that employed wearable or embedded physiological sensing in VR systems.

2.1 Physiological Sensing in VR

Since its early implementations, subjective measures have been the most common tool to evaluate VR experiences. However, several researchers have documented that when used alone, they are insufficient to describe the complex phenomena occurring in VR immersive experiences (cf. [38, 92, 95]). Physiological sensing addresses some significant shortcomings as they are implicit, online, and can provide continuous measures of autonomic functioning. Over the last years, researchers investigated physiological measures in VR, such as clinical applications [11], physiologically-adaptive VR systems [24, 26], evaluation of VR systems or parameters [75] by the acquisition of central and

peripheral physiological signals. When considering VR adaptation using physiological sensing, studies showed the viability of adapting to the user's emotional state [64], games narrative [44], or task difficulty [25].

Several studies explored the use of peripheral physiological measures, such as EDA and PPG. EDA refers to changes in skin conductance by activating eccrine gland activity, and it is a measure of sympathetic arousal with a long history of investigating users' emotional and cognitive states [63]. Given the capability of VR environments to trigger higher emotional and physiological arousal, EDA measures found diverse applications for investigating VR phenomena, interaction, and system adaptation [89]. EDA was shown to positively correlate with presence [10, 57], cybersickness [40], and illusion of body ownership [7, 34].

PPG employs pulse oximetry to detect blood volume changes in the microvascular bed of tissue [5]. It stems from the use in cardiology as a diagnostic tool for cardiac arrhythmia and heart failure [3] to applications in VR, given its practical implementation in wearable solutions as compared to electrocardiography (ECG) [48]. This increasing use of PPG is motivated by the fact that PPG sensors do not rely on electrical activity (i.e., they do not require conductive gels upon application) and that, under certain conditions, they can provide a measurement accuracy close to that of ECG in detecting cardiac activity measures such as HR or heart rate variability [77, 93]. Specifically, PPG has been widely exploited in online studies to classify users' states such as workload [29], anxiety [90], and stress [27]. In conclusion, EDA and PPG can be widely applied to physiologically estimate and monitor users' emotional and cognitive states in VR.

2.2 Wearable Physiological Sensing

The need to push forward the application of physiological sensing in VR requires multidisciplinary notions about both psychophysiological principles and technical integration of physiological signals in VR [4]. Unfortunately, such a need for implementation and synchronization within the VR environment is currently inconvenient as it relies on unpractical hardware-software solutions [83]. First, researchers must independently prepare and calibrate each sensing system when planning to acquire different physiological data, increasing the setup time. Second, when immersed in VR, users do not perceive their bodies nor the physiological sensing systems attached, causing possible disruptions by cables, VR tracking, or more. Third, such situations can impair signal quality resulting in artifacts or even signal loss, and disrupt the engagement within the virtual environment. This has led to the proliferation of plug-play, wearable and uncomplicated data collection solutions [67]. The availability and variety of easy-to-use wearable sensors promote physiological data acquisition for evaluation and adaptation purposes [26, 60].

The commercial-grade quality of these devices often implies a lack of access to raw data or exploitation of "black-box" proprietary metrics developed by the manufacturer. This has prompted many researchers to evaluate ad-hoc solutions involving integration within the VR system. Embedding physiological sensing within the VR environment presents several advantages: hardware and software are integrated into one single device allowing for improved comfort, low-cost implementation, and even improved acceptance [43]. Several embedded physiological sensing in VR headsets allow for gaze and eye-tracking [62], or even multiple physiological signal recording [14]. Bernal et al. [14] provided a "mask" with high-quality equipment for sensing different physiological signals, such as facial electromyography (sEMG), electroencephalography (EEG), EDA, and eye-tracking data in XR environments. While EEG and sEMG recordings benefit from the placement on the prefrontal cortex, frontalis, and zygomaticus muscles, EDA signals collected from the forehead showed weak correlations with tonic and phasic components from phalanx sites (i.e., most responsive sites in the human body), possibly due to their stronger sensitivity to thermoregulatory activity rather than physiological arousal [81]. Critically, none of the above devices has been validated in

ecological VR settings [20], with most of them having been compared with medical-grade devices only in controlled lab settings [77, 78]. Currently, most VR sensors are either embedded in the headset or do not feature any physiological measuring capacity in controllers as the main focus is on hand-motion and tracking systems [58]. The present work, therefore, aims to explore possible alternatives in integrating physiological measures of arousal into VR systems and validating them as reliable and accurate measures. We first conducted a study to identify optimal sites for EDA and PPG sensor placement embedded in a VR controller. Second, we evaluated the performance of SensCon across a variety of VR scenarios widely used in stress and psychophysiology research.

3 STUDY 1: FINGER PLACEMENT AND HAND GRASP DURING VR CONTROLLER INTERACTION

In the past, many inside and outside tracking methods have been pioneered to gain various states from the user, e.g., [1, 2]. However, the reason trends point towards inside tracking as the environment does not need to be equipped with technology allowing for improved flexibility and mobile applications. Thus, integrating physiological sensing into VR systems aligns with current trends in VR development. For example, recent research has explored the integration of cameras into VR controllers for optimal body and hand-tracking [2, 98], enabling the design of intelligent mobile standalone VR systems. This trend is already being implemented in commercial VR systems, such as the camera embedded in the Meta Quest Pro [16]. Second, while others showed that placing sensors in the headset is feasible (e.g., [70, 113]), when considering peripheral physiological measures such as EDA and PPG there are cautions to be taken for validation purposes. We wanted to maximize the signal agreement between SensCon and the gold standard measurements used in Study 2 (i.e., finger PPG and finger EDA), implying peripheral measures from the hand/finger. That is, using different measurement locations would have implied less fairly comparable measurements, also due to the higher eccrine sweat glands density in the hands compared to other body sites [100] and the different pulse transit time implied by hand and head PPG sites [91]. By embedding physiological sensors into VR controllers, we can enhance the user experience in VR environments and enable the design of novel physiologically-aware VR applications.

To ensure adequate sensor placement in the VR controller, we conducted a study to determine grasping location while holding an HTC VIVE controller and simultaneously pressing three key buttons (Trigger, Grip, and Trackpad buttons) following the approach by Le et al. [65]. We were especially interested in where the grasping hand made contact with the controller, which we analyzed by measuring the contact surface when participants grabbed the VR controller. We computed and analyzed the degree of overlapping across participants.

3.1 Procedure

First, we asked participants to handle the controller until they felt comfortable pressing the Trigger, Grip, and Trackpad buttons without moving their hands. Next, we outlined the participant's hand with a fine-pointed white pen. In this way, the contour of the participant's handprint was drawn on the VR controller. Next, the participant removed the hand from the controller to imprint it with colored paint on a flat plate to optimize the spread. The participant then held the VR controller, trying to follow the previously outlined contour, optimizing the grasping to press the buttons. Finally, the participant released the grip on the VR controller. The researcher then photographed the front, bottom, left, and right sides of the controller five times using a professional camera (Canon EOS 50D, 4752×3168 pixels) positioned on a solid stand that was kept constant throughout the photographs.

The controller was placed inside a 3D-printed holder on top of a table to ensure orthogonality for the axis of the table and the camera. We placed a QR code on each side for orthogonal image alignment processing to allow optimal perspective transformation.

3.2 Participants

The study was performed in a quiet and distraction-free environment, where participants sat and could focus on handling the controller. Twelve participants, six identified as female and six as male ($M_{age} = 27.5$, $SD_{age} = 2.74$) took part in the study. We asked participants to hold the controller with their dominant hand [52], with ten using their right hand and two using their left hand, respectively. We measured three standardized hands metrics following the guidelines of the Human Engineering Design Data Digest [86]: (I) handbreadth ($M_{cm} = 8.4$, $SD_{cm} = 0.32$), i.e., distance between the two metacarpal bones (metacarpal-phalangeal joints), (II) hand length ($M_{cm} = 17.98$, $SD_{cm} = 0.66$), i.e., distance from the base of the hand at the wrist crease to the tip of the middle finger and, (III) hand circumference ($M_{cm} = 18.91$, $SD_{cm} = 0.89$), i.e., circumference of the hand measured around the knuckles (metacarpal-phalangeal joints). In this way, we respectively covered 50^{th}, 95^{th}, and 99^{th} percentile for both men and women in hand measures as per the Human Engineering Design Data Digest [86].

3.3 Image Processing

We preprocessed the images using Python library OpenCV (Version 4.3) [17] and Adobe Photoshop (Version 23.4.2)[1]. We placed four QR codes on the front, back, and left and right side of the VR controller holder for coarse image alignment [56]. On such images, we applied a perspective transformation to align and overlap the QR codes from every side and, consequently, the pictures of contact locations on the VR controller. As a final step in the image processing phase, we applied Lens correction in Adobe Photoshop to all images using a distortion correction model to improve pictures' parallelism, size, and rotation. Next, we masked all areas where the fingers touched the controller, allowing us to calculate the area for each user.

3.4 Results

We extracted the area touched by participants during the comfortable holding of the controller. For this, we aligned the areas touched and measured the area which could theoretically be touched (the shaft of the controller). We found that 64.1% of the front, 73.1% of the back, 87.1% of the right side, and 57.1% of the left side will be touched by at least one participant, see Figure 1. While this is a good first indication of surface coverage, we next calculated the area which was touched by all 12 participants for successful sensor placement. Here, we found that 14.1% of the front, 11.3% of the back, 47.8% of the right side, and 5.4% of the left side were touched by all participants. The area with the perfect overlap is shown in Figure 1c – the middle of the right side of the controller.

Of note, such images are from the perspective of holding the controller on the right side. However, due to the symmetric anatomy of the human hand, the results for the left hand are the same but mirrored. As such, we can say that the optimal area for a sensor is not per se on the right side of the controller but where the palm of the hand touches the controller (right side for the right hand and left side for the left hand, respectively).

(a) Front (b) Back (c) Right (d) Left

Fig. 1. Heat maps showing the area of the VR controller with the highest contact overlap during interaction in Study 1.

Fig. 2. The schematic overview of the SensCon. Data are acquired via PPG and EDA sensors in the VR controller. Physiological data are streamed within a UDP protocol to the experiment control PC. Finally, the VR environment is displayed to the user via a wired HTC VIVE headset.

4 THE SENSCON SYSTEM

With SensCon, we combine commodity VR controllers with PPG and EDA sensors for a wide range of future applications using physiological sensing and thus, adapt to the users' state. We used two HTC Vive controllers as a base to host the sensors to accomplish this.

4.1 Hardware Implementation

Based on our results from Study 1, we considered that a sensor with a low surface area, such as a PPG sensor, would have been best placed on the right side of the controller, or in other words, below the palm of the hand, see Figure 3. Finally, we noted that the left side of the controller consisted of a large surface while not being constantly covered by the fingers. Thus, we selected it as the ideal location of the second EDA electrode. In sum, we mounted the two EDA electrodes on both sides of one controller (see Figure 3) and the PPG sensor on the well-covered right side of the second controller, respectively (see Figure 3).

[1]https://www.adobe.com//products/photoshop.html

Fig. 3. EDA and PPG sensors integrated into VR controllers. In the first picture, EDA sensor is integrated into a controller. In the second figure, two copper stripes measure the EDA when a user picks up the controller. In the third figure, PPG sensor integrated inside the controller. In the fourth figure, the PPG sensor measures the user's HR by implicitly pressing the palm against the sensor.

With this goal in mind, we integrated the PPG and EDA sensors into two HTC Vive controllers. For the communication and local sensor control unit, we used an ESP 8266 D1 Mini[2] microcontroller offering both WiFi and Bluetooth connectivity. Thus, we sent the PPG and EDA data via a WiFi and UDP connection to a Lab Streaming Layer[3] (LSL) server for signal time synchronization and data logging via Arduino. Figure 2 shows the schematics of SensCon. We also added an additional micro-USB port on the underside of the VR controller (see **??** and **??**), allowing for fast deployment of updates and acting as a debug terminal.

The controllers have built-in batteries with 960mAh at 3.85V. However, this is under the minimum required 4V for the V_{in} of the microcontroller. Thus, we incorporated a "step-up DC" in the controller while losing playtime by draining the built-in battery. Thus, we opted to add a power bank connected to the ESP flash port instead. Pulse Sensor PPG and Groove GSR sensors required a stable power consumption of $.08A$, as measured via a USB digital multimeter. We allowed for long playtime and easily swappable batteries.

4.2 Sensing EDA

We use a Groove galvanic skin response (GSR) sensor[4] to measure EDA with a sample rate of 192 Hz. First, we disassembled an HTC Vive Controller and integrated the sensor in the handle (see Figure 3). We then soldered the pins of the connectors to two pieces of copper band that we adhered around the handle (see Figure 3). The resistance between the contacts is measured in one hand by closing the two copper contacts when taking the controller into the hand. The GSR sensor captures micro voltages (μV) between the distal phalanges as a measure of skin resistance utilizing the µV input in Ohms (Ω). The formula for skin resistance computation is provided by the manufacturer

[2] www.openhacks.com/uploadsproductos/tutorial_nb.pdf
[3] https://github.com/sccn/labstreaminglayer
[4] https://wiki.seeedstudio.com/Grove-GSR_Sensor/

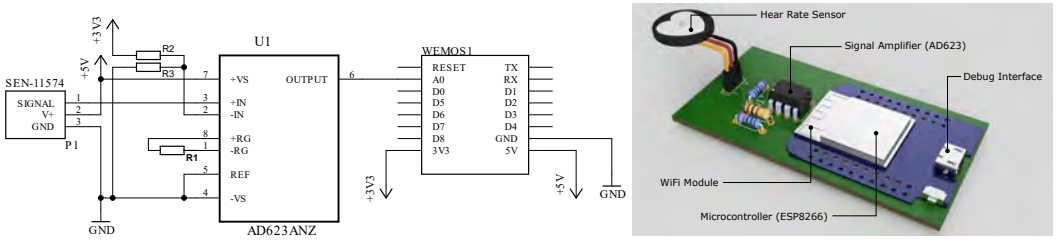

(a) Circuit Schematic (b) 3D Model

Fig. 4. PPG signal conditioning: we employed an instrumentation amplifier to increase the amplitude of the sensor's raw signal. This configuration utilizes a voltage divider, with the gain regulated by a single resistor (R1). Specifically, (a) depicts the circuit powered by the WEMOS D1 mini platform, which integrates an ESP8266 micro-controller. The heart-rate sensor's signal is processed by the AD623 instrumentation amplifier and subsequently transmitted to the WEMOS platform. Alternatively, (b) illustrates the circuit diagram and its various components.

and shown in Equation 1:

$$SR(\mu\Omega) = ((1024 + 2 * \mu V) * 10,000)/(512\mu V) \tag{1}$$

Therefore to compute EDA, we computed the reciprocal of resistance, i.e., conductance, measured in (μS) as in Equation 2:

$$EDA(\mu S) = (512\mu V)/(\mu\Omega) = ((1024 + 2 * V) * 10,000) \tag{2}$$

4.3 Sensing PPG

We integrated a Pulse Sensor[5] by punching a circle-shaped hole located at the palm hand position of the controller (see Figure 3). We placed the Pulse Sensor on the left side of the HTC VIVE controller as depicted in Figure 3. In this location, we allowed for 100% of surface overlapping across participants. Then, we disassembled a controller to integrate the D1 mini microcontroller, and we connected it to the PPG sensor.

The Pulse Sensor is an optical HR sensor (i.e., PPG) that features on the frontal side of the sensor, an APDS-9008 Light Photo Sensor, and a reversed mount LED. In this way, the reflected green light ($\sim 550nm$) from the LED through the fingers is measured via the photosensor. On the back of the module, an MCP6001 Op-Amp microchip consists of three resistors and capacitors that form an R/C filter circuit. This circuit is used for noise cancellation and amplification to avoid time delay in pulse recordings. The module operates from a 3.3 to 5V DC Voltage supply with an operating current of 4mA. The desired sampling rate is set at 250 Hz.

4.4 Open Source

We open-sourced the full implementation of SensCon. First, we provided a list of the materials needed to implement SensCon. Second, we provided the schematics for the electronics housed in the VR controllers. Third, we provided a manual to assemble SensCon. Fourth, we open-sourced the code to retrieve the sensor data and send it onto the LSL stream. Finally, we provided a Unity package to receive the real-time LSL stream[6].

[5] https://pulsesensor.com/
[6] https://github.com/mimuc/Senscon/

5 STUDY 2: SYSTEM EVALUATION

Study 2 aimed at assessing the UX and measurement accuracy of SensCon, as compared to medical-grade devices measuring EDA and PPG-based HR. We divided the description of the study into two parts. The first part investigates usability, acceptance, and UX by letting users freely use either SensCon or VR controllers with attached medical-grade equipment, and by collecting subjective measures using questionnaires after each condition.

The second part evaluates the measurement accuracy across the included VR tasks. That is, it presents a within-subjects study focusing the agreement between SensCon and medical-grade physiological sensors. The following research questions guided our evaluation:

RQ1 Does an embedded physiological sensing system provide higher usability and UX in VR environments when compared to medical-grade devices?

RQ2 Does an embedded physiological sensing system allow for comparable signal quality and outcome measures to those obtained with medical-grade devices?

5.1 Independent Variable: Physiological Sensing System

We considered the physiological sensing systems, consisting of SensCon and the medical-grade devices as the only independent variable for both parts of our study. We evaluate if the sensors integrated into SensCon can act as a usable alternative to medical-grade devices (i.e., PPG finger-clip sensor and EDA Ag/AgCl electrodes measured from the index and middle fingers) over six different tasks.

5.2 Measurements

The first part of the study focused on the usability, acceptance, and UX aspects in the first part of the study. Participants were equipped with either SensCon or medical-grade devices while walking around. Then, after using each system, they filled in three self-report scales. We started with the System Usability Scale (SUS) [66] questionnaire to measure system usability. We then proceeded with the Unified Theory of Acceptance and Use of Technology (UTAUT) [104] questionnaire to assess the acceptance of the two systems. Finally, we administered five seven-point Likert items to obtain an overview of the UX using the physiological sensing systems. The self-report scales are depicted in Table 1.

In the second part of the study, we measured both EDA and HR using SensCon and the medical-grade devices at the same time throughout six different tasks. SensCon measures EDA upon making contact with the user's left hand while the medical-grade device obtains the measures by clipping two Ag/AgCl electrodes on the index and middle finger of the same hand. For EDA data acquisition, we followed the guidelines for HCI community by Babaei et al. [8]. SensCon obtains the PPG signal from the user's right hand's palm. The medical-grade device assesses the PPG through a finger clip placed on the index finger.

5.3 Apparatus

For the medical-grade recordings, we chose the GSR module (BrainProducts GmbH, Germany)[7] and blood pulse sensor for finger PPG (Nellcor DS-100A, Nellcor, USA)[8] as the gold-standard physiological sensing systems. Those are two sensors within a computerized recording system that encodes up to eight channels with a sampling frequency of up to 1000 Hz. Both devices are shown in Figure 5. To achieve optimal time synchronization across measures, both physiological

[7] https://www.brainproducts.com/files/public/sensor-tutorial/Content/Topics/1.GSR/Acquisition/LiveAmp%20GSR.htm
[8] https://www.brainproducts.com/files/public/sensor-tutorial/Content/Topics/2.Photoplethysmogram/Acquisition/LiveAmp%20PPG.htm

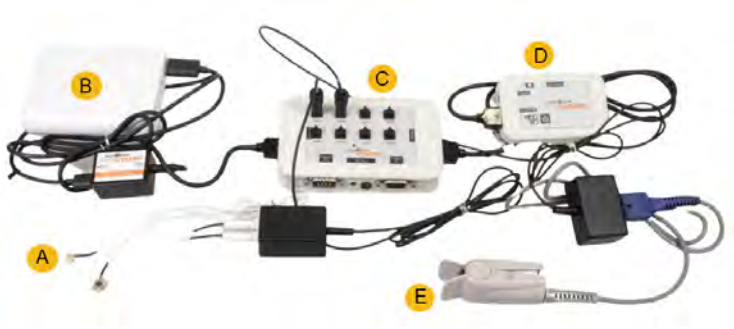

Fig. 5. The medical-grade system used as gold standards for evaluating SensCon-based EDA and PPG measurements. The EDA electrodes (A) and PPG finger clip sensor (E) are connected to the AUX ports of the Sensor & Trigger extension (STE) (C). For signal amplification and streaming to the acquisition PC, we use a LiveAmp amplifier (D) and a power bank for energy supply to the STE (B). All components were placed inside a pouch and comfortably worn by participants across the experimental sessions

sensing systems are connected to the Stimulus and Trigger Extension (STE; BrainProducts GmbH, Germany). We acquired and synchronized the signals at 250 Hz. Therefore, this study considers the GSR module and the PPG finger-clip sensor the gold standard measurement devices.

For the SensCon recordings, we integrated an EDA (see Section 4.2) and a PPG sensor (see Section 4.3) into two separate HTC Vive controllers. The controller containing the EDA sensor was held with the participant's left hand, while the controller with integrated PPG was held with the right hand. Prior to analyzing the data, we calibrated each PPG measurement by subtracting an estimate of the mean offset (i.e., the systematic difference) between the two PPG signals acquired from the medical-grade device and SensCon. This was done by using data recorded in seated resting conditions from three further participants (M_{age} = 25, SD_{age} = 2.45) that were not included in the main sample for Study 2. We obtained an average offset of 11.1 bpm (SD = 12.1), which was used to correct the signal acquired from SensCon. All collected data of SensCon and the medical-grade equipment were then sent over the network and synchronized on the same computer using LSL. We used an HTC Vive to display the virtual environments in the second part of the study. The participants' movements were tracked using two VIVE lighthouses.

Table 1. Seven-point Likert questions used to assess the user experience and pleasantness of both SensCon and the medical-grade sensors.

ID	Question
Q1	*It was very comfortable to use the system.*
Q2	*It was very annoying to use the system.*
Q3	*It was very pleasant to use the system.*
Q4	*It was very difficult to use the system.*
Q5	*I want to use the system in my everyday VR experiences.*

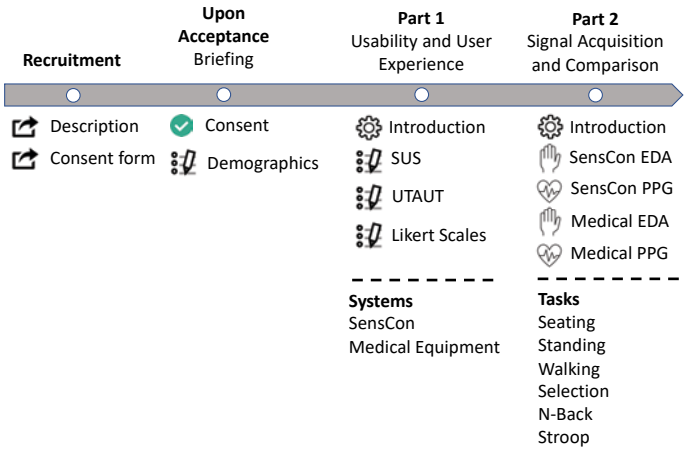

Fig. 6. Graphical description of the study procedure. The study consisted of two parts assessing the user experience and signal quality, respectively.

5.4 Procedure

Upon arrival, participants received a written briefing on the experimental procedure and provided their informed consent. Afterward, they provided their demographic data, including age, self-identified gender, weight, and height. We then started with the first phase of the study to compare the usability of SensCon and the medical-grade devices. In two separate conditions, participants were either equipped with SensCon or both the EDA and PPG medical devices without being immersed in the VR environment. We asked participants to walk around with the hardware and perform several actions, including hand movements and pointing gestures. Then, participants filled in the SUS and UTAUT scales and the custom Likert items to assess the UX. The same procedure was repeated for the other physiological system modality, and the order presentation of physiological sensing devices was counterbalanced across participants.

The second part of the experiment evaluated the signal quality between SensCon and the medical-grade devices. We instructed the participants to hold the SensCon controllers in their hands while the medical-grade devices were simultaneously applied (i.e., EDA on the left index and middle finger, PPG fingerclip on the right index finger). Before data acquisition, the participants were seated and were allowed to visually explore the VR scene for two minutes by moving their heads. Then, participants started to engage in the six experimental tasks while the physiological signals were recorded in real-time. The procedure of the study is illustrated in Figure 6

5.5 Tasks

We used established tasks that have been shown to elicit traceable changes in autonomic responsiveness and particularly in the signals of interest [18]. We implemented the six tasks using Unity3D, and we used an HTC Vive headset to visualize the environment (see Figure 7). In between the tasks, participants underwent a break of six minutes to allow for physiological re-adaptation (i.e., recovery to the basal physiological levels). The six tasks described below were performed in the same following order by all participants.

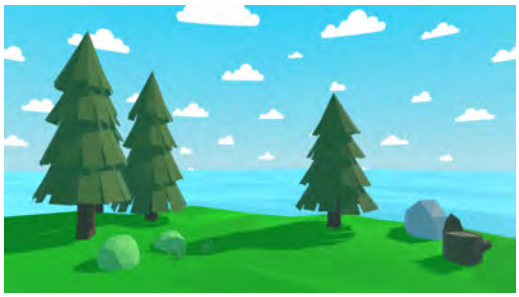

(a) Seating, standing, and walking task.

(b) Selection task.

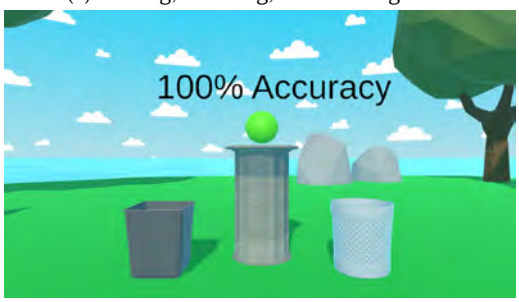

(c) N-Back task.

(d) Stroop task.

Fig. 7. The six different tasks of our validation study. Each task had a total duration of three minutes and was performed one after the other. The first five tasks took place in a low-poly environment while the Stroop was performed in a separate virtual room.

5.5.1 Seating. Participants were comfortably sitting on a chair while immersed in the VR environment (see Figure 7a). They were asked to position their hands on their thighs without moving them while holding the controllers in their hands. We chose this condition as seating rest has been recommended and widely used as a baseline condition in previous research [18].

5.5.2 Active Orthostatic Test. The active orthostatic test evaluates the effects of sudden postural changes and it is often used to assess autonomic responsiveness [47]. This condition was shown to affect PPG measures in previous research [21, 68, 77, 82]. Participants were required to stand and maintain an upright position over three minutes in the VR environment.

5.5.3 Slow Walking. Participants were asked to naturally walk along a path designed in the VR environment to maintain an upright position. That is, they walked over a guidance line in the virtual environment. This task was designed to evaluate the effect of natural body movement on data quality, as done in previous studies [77].

5.5.4 Selection Task. Participants were required to select yellow spheres and red cubes within a selection task. Then, they must touch the yellow sphere with the left VR controller and the red cube with the right controller, see Figure 7b. Spheres and cubes were randomly presented in a sequence. The movements were sequentially guided. This task was included to test the influence of hand movements on the signal quality together with the general movement of the entire body.

5.5.5 VR N-Back Task. The N-Back task is an established task that recruits working memory resources and thus, evokes physiological and psychological stress responses [42]. It has been used in psychophysiological research with both healthy [85] and clinical populations [50]. We adapted

the VR N-Back task from Chiossi et al. [25], requiring participants to place a sphere, which was initially presented over a pillar, into one of two different baskets. The sphere should be placed in the right basket when it had the same color as the sphere presented N times before, whereas when the color was different, the sphere should be placed in the left bucket. The N-Back level (i.e., N refers to the amount of steps, in this case spheres, in the sequence) was set at 2. To keep the level of engagement high, we showed an accuracy index based on the last 20 balls placed, and participants were asked to maintain a performance index above 90%, see Figure 7c.

5.5.6 VR Stroop Task. The Stroop task is an established paradigm that investigates cognitive control and interference (i.e., inhibition of automatic behavioral responses due to a color-word interference) [108]. In addition, it is widely used in psychophysiological research as a cognitive stress test eliciting autonomic responses [9]. We used the VR concept proposed by Gradl et al. [45] as it was shown to elicit increased levels of HR and EDA indicators. In this VR version of the Stroop task, participants were surrounded by six walls "painted" in a changeable color and they were asked to select the wall color matching the feature of interest (i.e., either color or word). For example, in incongruent trials, if the word "Green" was colored in yellow and the color was the relevant feature, then participants shoud select the yellow wall with the controller, see Figure 7d. In contrast, if the COLOR is the relevant feature, they should select the purple wall.

5.6 Participants

Twelve participants, six identified themselves as female and six as male (M_{age} = 30, SD_{age} = 1.81), voluntarily participated in the study. None of the participants had a medical history of psychiatric or neurological diseases, color blindness or not assuming medications affecting the autonomic system. All participants provided written informed consent and received a monetary compensation of 10 Euros. Participants were required to avoid practising strenuous physical exercises, smoking, and consuming coffee over the three hours before the experimental session.

6 RESULTS

First, we evaluated the measurement accuracy of two sensors for measuring EDA and HR embedded in a VR controller across tasks. We used frequentist factorial analysis of variance (ANOVA) or ART ANOVAs [109] accounting for the non-normality of the data distributions. Moreover, to draw meaningful information from null results, we also reproduced the analyses with a Bayesian approach [102]. That is, we performed a Bayesian ANOVA using default Cauchy's priors and 10,000,000 iterations with Task and participant as random effects.

Second, we better evaluated the agreement between SensCon-based measurements and those obtained with the corresponding medical-grade devices by means of Bland-Altman analyses [6, 15].

Table 2. An overview of dependent variables analyzed via factorial ANOVA or ANOVA ART and Bayesian ANOVA.

	Frequentist Testing					Bayesian Testing	
	Normality		System				
	W	p	F	p	η^2	BF_{10}	$Error$
nsSCRs freq.	.794	<.001	.109	.741	.001	.380	.24
SCL	.917	<.001	.257	.613	.003	.348	.21
HR	.987	.328	.765	.405	.012	.876	.14

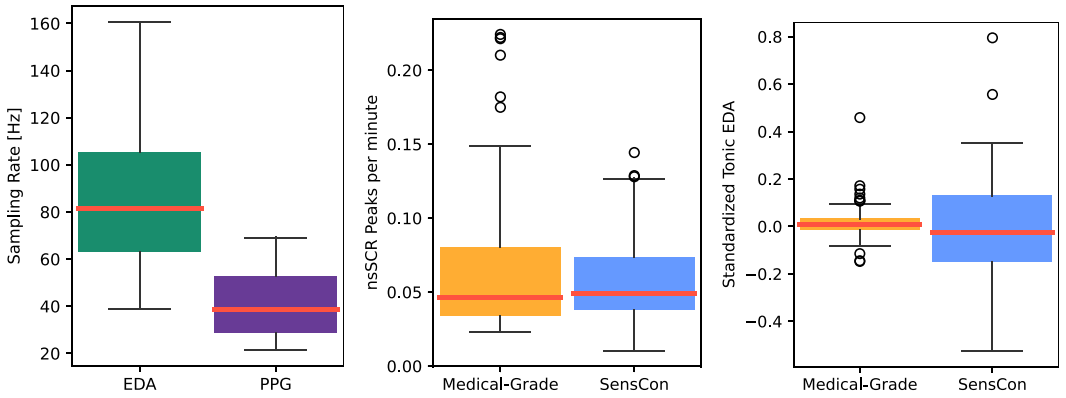

(a) Sampling Rate (b) nsSCRs (c) SCL

Fig. 8. Results for signal accuracy for SensConEDA. a) the actual sampling rate of SensConEDA. b) the nonspecific SCR (nsSCR) detected peaks per minute. c) the standardized tonic EDA acquired with both systems.

Bland-Altman plots and related statistics are the most established analytical tool for comparing two methods providing quantitative measurements, and they are widely used to evaluate how accurately a new method measures a specific signal compared to a reference method. In Bland-Altman analyses, measurement accuracy is established as the agreement between the new method (here, SensCon) and the gold standard (here, medical-grade devices), expressed in terms of systematic bias and random error. The former represents the most likely difference to occur, whereas the latter quantifies the range within which most differences are expected to lie, as indicated by the limits of agreement (LOAs) [73]. Specifically, we conducted separate analyses for each signal and task following the procedures described by Menghini et al. [76]. That is, we accounted for cases of proportional and heteroscedastic differences by representing bias and LOAs as a function of the range of measurement. Both bias and LOAs were computed with their 95% confidence intervals based on parametric bootstrap with 10,000 replicates. Bland-Altman analyses supersede classic correlation analyses as the latter only describes the linear relationship between measures but not their agreement, possibly providing misleading results [41], especially considering that data with high correlations might result in a low rate of agreement [33]. Thus, while we report correlations in the appendix (Table 4 and Figure 15), we grounded our work on Bland-Altman analyses.

Finally, we supplement the results coming from our validation analysis with t-tests or Wilcoxon tests for each self-report scale, i.e., Usability (SUS), Acceptance (UTAUT), and Likert Scales on UX.

6.1 Electrodermal Activity

EDA data both from gold-standard device and SensCon were processed using the Neurokit Python Toolbox [72]. We first applied a 3 Hz, high-pass, fourth-order Butterworth filter to remove high-frequency noise. We then decomposed the signal into tonic and phasic components by using the non-negative deconvolution analysis [13]. Lastly, we extracted peaks from the decomposed signal using a threshold value of $0.05\mu S$ [37]. These preprocessing steps allowed us to compute the average SCL and the mean frequency of not specific SCRs [19].

First, we analyzed the reliability of the acquired signal. Here, we calculated the effective sampling rate and found that the EDA sensor delivers samples on average with 86.7 Hz (SD = 29.5Hz, min = 38.6, max = 160.5), see Figure 8a.

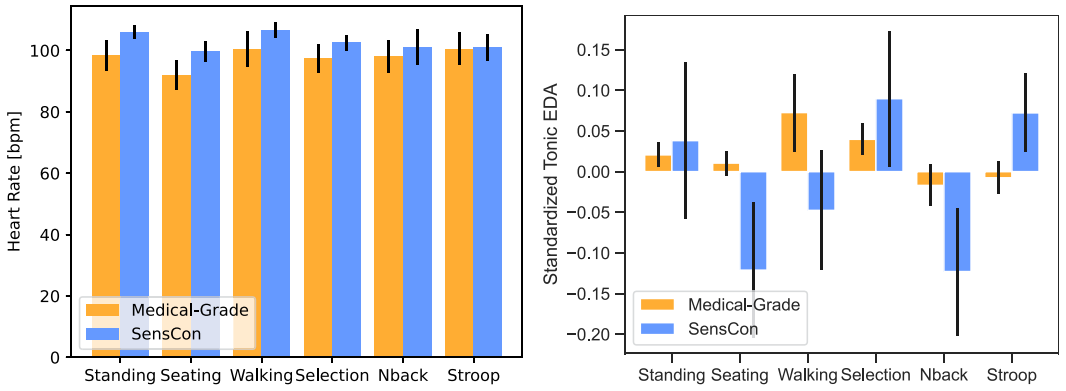

(a) HR (b) SCL

Fig. 9. Mean HR (a) and Mean SCL (b) across Tasks for SensConand medical-grade devices. Differences computed between SensConand Medical Grade devices for HR and EDA Tonic were not significant.

We analyzed the signal in the time domain based on the recorded data by comparing their standardized signals. First, we analyzed the nonspecific SCRs (nsSCRs) peaks per minute. As the normality assumption was not met (Shapiro-Wilk: $W = .794$, $p < 0.001$), we relied on ART ANOVA [109], showing no significant differences between systems in *nsSCRs* after controlling for Task ($F(1, 99) = 0.109$, $p = .741$), see Figure 8b. A Bayesian ANOVA indicated anecdotal evidence for the null hypothesis H0 ($BF_{10} = .380$) with Task and participants as random factors.

Finally, we computed the standardized SCL, accounting for interindividual differences [12, 71, 101]. As the normality assumption was not met ($W = .917$, $p < 0.001$), we relied on ART ANOVA [109], showing no significant differences between systems in *nsSCRs* after controlling for Task ($F(1, 99) = 0.257$, $p = .613$), see Figure 8c and 9b. A Bayesian ANOVA indicated anecdotal evidence for H0 ($BF_{10} = .348$) with Task and participants as random factors.

6.2 Photoplethysmography

We based our evaluation on PPG-related measures in the time domain, focusing on HR. As with EDA, the measured PPG values were processed using the Neurokit Python Toolbox [72]. We first applied a third-order Butterworth filter from 0.5 to 8 Hz.

We analyzed the availability of the signal. Here, we calculated the effective sampling rate and found that the PPG sensor delivers samples on average with $41.4Hz$ ($SD = 13.7Hz$, $min = 21.5$, $max = 69.1$), see Figure 8a.

For the HR analysis, we computed the overall differences between SensCon and the medical-grade devices. As the normality assumption was met ($W = .987$, $p = .765$), we relied on the ANOVA, showing no significant effect of System on *HR* after controlling for Task ($F(1, 9) = .765$, $p = .405$), see Figure 9a. A Bayesian ANOVA indicated no evidence for H0 ($BF_{10} = .876$) with Task and participants as random factors.

6.3 Bland-Altman Analysis

6.3.1 Electrodermal Activity. Bland-Altman statistics for SCL and nsSCRs are reported in Table 5 in the Appendix and the corresponding Bland-Altman plots are visualized inFigure 10 and Figure 11. SCL showed proportional biases in most tasks, implying that the magnitude of the differences between systems was dependent on the size of the measurements. In the Seating, Standing, Selection,

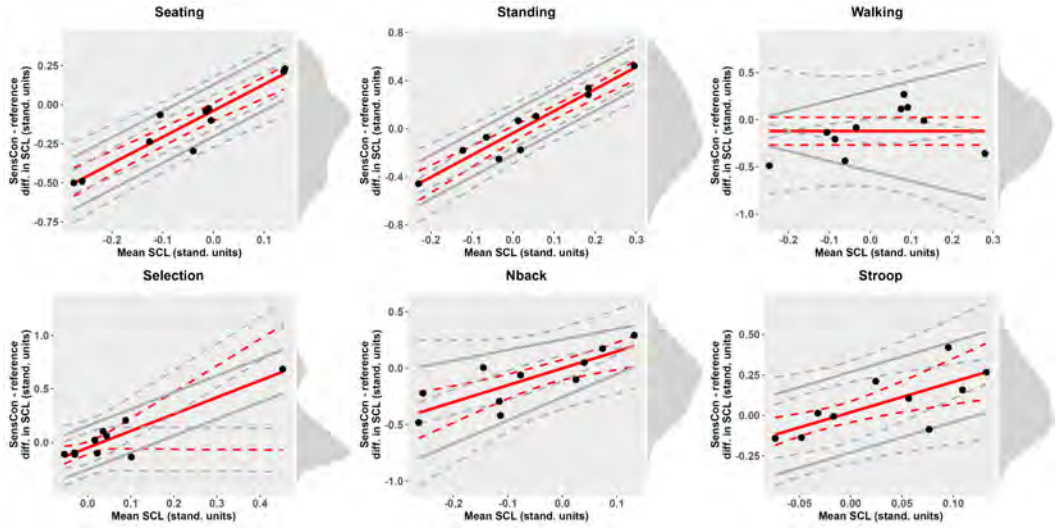

Fig. 10. Bland-Altman plots for standardized SCL during Seating, Standing, Walking, Selection, N-Back and Stroop task Solid red lines show the bias (i.e., mean difference) and the 95% limits of agreement (LOAs). Gray dashed lines show the associated 95% confidence intervals.

and Stroop tasks, SensCon showed the highest accuracy for intermediate SCL values, whereas it systematically underestimated lower SCL values and overestimated higher values, respectively. In contrast, only relatively high SCL values were measured without bias in the N-back task, showing underestimations for lower SCL values. The Walking task was the only condition showing uniform and nonsignificant bias, although we found wider LOAs for higher SCL values (i.e., heteroscedasticity). Heteroscedasticity was also detected in the N-back task but in the opposite direction, with higher random error for lower SCL measurements. Critically, in most tasks the computed LOAs were wider than the range of measurement, suggesting that SensCon-implied random error in SCL measurement might be too large, at least for extreme values.

A similar scenario was found for nsSCRs, showing uniform and nonsignificant bias only in the N-back and the Stroop task, whereas negative proportional biases were found in all the remaining tasks. Specifically, in the Seating, Standing, Walking, and Selection tasks SensCon showed the highest accuracy for lower rates of nsSCRs, that is when participants showed no or only a few responses, whereas it tended to underestimate larger nsSCRs measurements compared to the medical-grade device, possibly indicating false negatives. Higher nsSCR rates were also associated with wider LOAs (i.e., positive heteroscedasticity) for the Standing, N-back, and Stroop tasks, with the latter requiring logarithmic transformation to improve data normality [36]. Again, LOAs were found to overcome the range of measurement for certain values, particularly for higher nsSCR rates.

6.3.2 Photoplethysmography. A better agreement was found between SensCon-based HR measurements and those obtained with the corresponding medical-grade device. As shown in Table X and Figure 12, uniform and not significant biases were found in all tasks, with negligible systematic differences between systems ranging from 0.2 to 7.56 bpm. However, the random component of measurement error was relatively high (i.e., around ±20-to-30 bpm). LOAs were uniform in most tasks, whereas negative heteroscedasticity was found in the N-back task, showing wider LOAs for

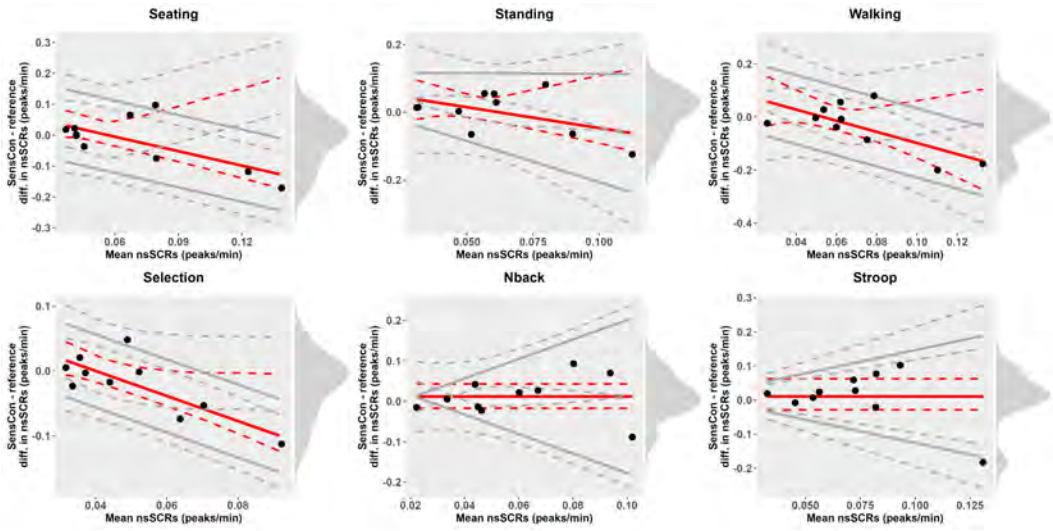

Fig. 11. Bland-Altman plots for average nsSCRs peak frequency during Seating, Standing, Walking, Selection, N-Back and Stroop task Solid red lines show the bias (i.e., mean difference) and the 95% limits of agreement (LOAs). Gray dashed lines show the associated 95% confidence intervals.

lower HR measurements. Slighter heteroscedasticity also characterized the Selection task, following the logarithmic transformation of the data to achieve normality [36].

6.4 Questionnaires

Finally, we tested the differences between SensCon and medical-grade devices considering the three self-report measures. Each measure was analyzed using t-tests or Wilcoxon-test upon normality testing. An overview of the results can be found in Table 3.

6.4.1 System Usability Scale. We aggregated the ten SUS items as recommended by previous research [66]. We conducted a Wilcoxon test as the Shapiro-Wilk test of normality showed a significant result ($W = 0.84$, $p < .001$), resulting in significantly higher usability for SensCon compared to the medical-grade devices ($W = .0$, $p < .001$). Figure 14a shows the mean score for both conditions.

6.4.2 User Acceptance. We analyze the eight UTAUT items by calculating the sum of the scales for each item [104]. As shown in Table 3 and Figure 13, we found significant differences in *Performance Expectancy*, *Effort Expectancy*, *Attitude Toward Using Technology*, *Behavioral Intention*, and *Anxiety*, but not in *Facilitating Conditions* and *Efficacy*.

6.4.3 User Experience. We analyzed the seven-point Likert scales by comparing each of them between the two systems. As shown in Table 3 and Figure 14b, we found a significant difference between all Likert scales.

7 DISCUSSION

Our results show that SensCon is an affordable alternative to medical-grade devices when it comes to measuring EDA and HR without compromising the user experience. Furthermore, SensCon empowers researchers and developers to obtain in-situ measurements of usability to assess the user experience in real-time or provide adaptive environments. Embedding physiological sensing

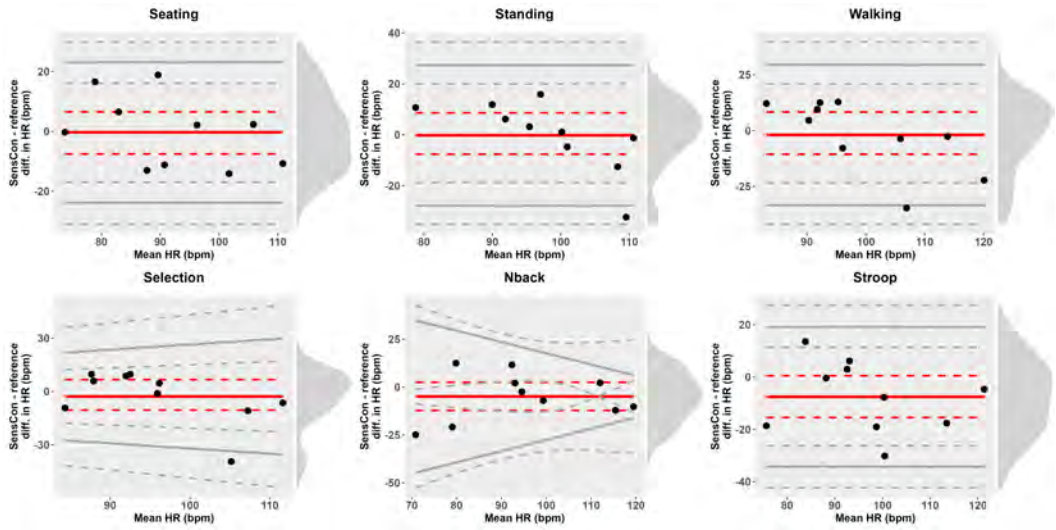

Fig. 12. Bland-Altman plots for mean heart rate during Seating, Standing, Walking, Selection, N-Back, and Stroop task Solid red lines show the bias (i.e., mean difference) and the 95% limits of agreement (LOAs). Gray dashed lines show the associated 95% confidence intervals.

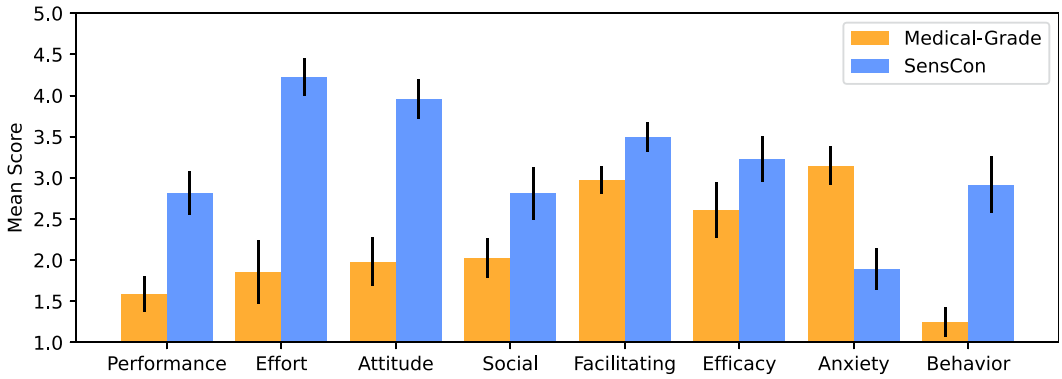

Fig. 13. The Acceptance (UTAUT) for SensCon was better evaluated across Performance, Effort, Attitude, Behavioral Intention, and Anxiety subscales than medical-grade devices.

for arousal detection into VR systems showed to allow for improved system UX and signal quality that did not show statistical differences for EDA and PPG extracted measures. We discuss the implications of our results in the following.

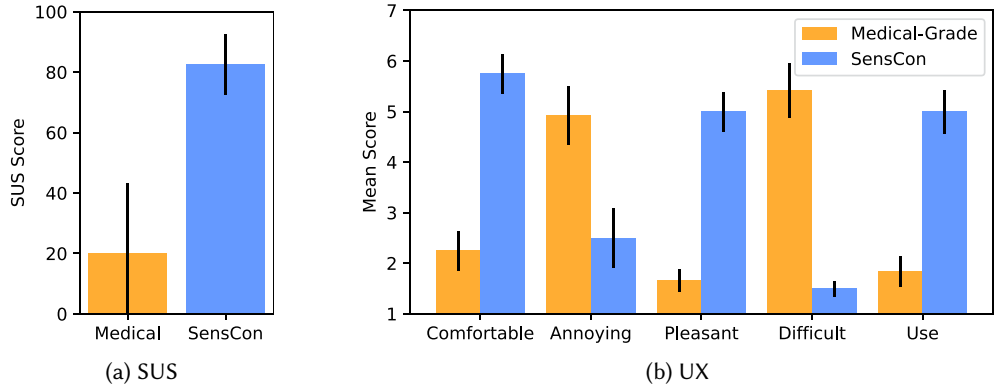

(a) SUS (b) UX

Fig. 14. Results for SUS questionnaire (a) and UX survey scoring for SensCon and the medical-grade devices. Results from UX survey (B) are aligned with the ones from SUS, showing that SensConwas better evaluated in terms of Comfort, Annoyance, Pleasantness, Difficulty to Use, and Intention to Use. Here, error bars denote the standard error.

Table 3. Statistical results of the SUS, UTAUT, and Likert questionnaires.

	SensCon		Medical		Normality		Test	
	M	**SD**	**M**	**SD**	**W**	**p**	**t/W**	**p**
SUS	82.5	9.6	20.0	22.2	.843	.002	0.0	**<.001**
Performance Expectancy	2.8	0.9	1.6	0.7	.907	.03	0.0	**.005**
Effort Expectancy	4.2	0.7	1.9	1.3	.843	.002	1.0	**.004**
Usage Behavior	4.0	0.8	2.0	1.0	.929	.092	−4.577	**<.001**
Social Influence	2.8	1.1	2.0	0.8	.890	.013	0.0	**.027**
Facilitating Conditions	3.5	0.6	3.0	0.6	.933	.116	−2.092	.06
Efficacy	3.2	0.9	2.6	1.1	.888	.012	12.5	.125
Anxiety	1.9	0.8	3.1	0.8	.926	.08	4.146	**.002**
Behavioral Intention	2.9	1.1	1.2	0.6	.808	<.001	0.0	**.005**
Q1: Comfortable	5.8	1.3	2.2	1.3	.839	.001	0.0	**.004**
Q2: Annoying	2.5	1.9	4.9	1.9	.810	<.001	5.0	**.012**
Q3: Pleasant	5.0	1.3	1.7	0.7	.901	.023	0.0	**.003**
Q4: Difficult	1.5	0.5	5.4	1.8	.812	<.001	0.0	**.003**
Q5: Like to Use	5.0	1.4	1.8	1.0	.898	.020	2.5	**<.001**

7.1 Usability-Friendly Physiological Sensing

Our results show that SensCon, as a physiological sensing system, is preferred from a usability perspective. Furthermore, probing the participants with different questionnaires revealed a preference to use SensCon over traditional medical-grade equipment from different aspects (i.e., SUS, Performance Expectancy, Effort Expectancy, Attitude Toward Using Technology, Self-Efficacy, Anxiety, and Likert scales concerning user experience). Hence, we are confirming **H1**.

Our findings indicate that integrated physiological sensing leads to higher user acceptance. Similar to devices known from the wearable computing area, the user acceptance of novel sensing

modalities increases when being integrated into everyday objects, hence increasing the quality of the overall interaction [55]. However, dealing with additional hardware to enable physiological interaction is often considered a burden by the user unless the obtained benefits overweight the workload of setting up a physiologically interactive system. SensCon overcomes these disadvantages by integrating physiological sensing into common VR controllers, leading to improved results regarding usability and user experience. However, it is important to acknowledge that medical-grade devices were designed for various purposes other than interactive VR systems only. Our results show that the adoption of physiological-interactive systems can be improved through direct integration into hardware. Consequently, we envision further research integrating alternative sensing modalities into VR controllers.

7.2 Signal Quality between SensCon and Medical-Grade Devices

The comparison of the aggregated EDA and PPG measurements between SensCon and the medical-grade equipment showed converging trends. In both cases, the mean differences evaluated via frequentist and Bayes showed non signifcant results and moderate to anectodal evidence for H0, i.e., claim that no difference exists between SensCon and Medical-Grade devices data distributions. Specifically, this applied for all the extracted measures of physiological arousal, i.e., SCL, nsSCR rate, and HR. This result is interesting cause shows that SensCon detected slow, such as SCL and HR, and fast changes in the arousal state of the user with similar data distributions as medical-grade devices.

However, a deeper look at the agreement between SensCon and medical-grade devices revealed that the measurement error implied by the former might be excessively high in some cases. Specifically, we found a tendency of SensCon to systematically underestimate nsSCR rate as the number of nsSCR peaks increased. Whereas this may indicate a low SensCon sensitivity to sudden EDA spikes, the analysis of SCL suggested that both extremely low and extremely high SCL measurements are systematically biased. Accounting for these specific cases that require further investigation with larger samples, our findings indicate a promising overall accuracy of SensCon in measuring tonic and phasic EDA under most conditions. However, future developments are needed to reduce the random error components of SensCon measurements. Indeed, whereas systematic biases were satisfactorily low in most cases (e.g., no systematic under- or overestimation was found for HR measurements), LOAs were relatively wide, especially for EDA measurements.

Although SensCon does not provide the same signal quality compared to medical-grade devices, it provides an alternative when usability and user experience are the focus of a physiological interactive system. We postulate a trade-off between sensing accuracy and the provided user experience. Reflecting on the not significant mean differences between the SensCon and medical EDA measurements, as well as the similarity between the SensCon and medical heart rate measurements, we can partially confirm **H2**.

SensCon provides an affordable and usable alternative for measuring physiological arousal at lower reliability compared to medical-grade devices. Although SensCon is providing less reliable data, future physiological interactive systems can observe the data over a period of time to selectively do an assessment of the perceived user experience and adaptations when a specific accuracy is reached. Past research recommends avoiding immediate adaptations to reduce the risk of damaging the user experience through maladaptations [99]. Instead, physiological data should be collected over a longer period to account for variations over time [54, 87]. SensCon can use this to its advantage by analyzing individualized physiological data over long periods, making predictions more robust for individual users. The technical contribution of SensCon will allow large-scale data collection to enhance long-term physiological interaction in virtual environments without compromising the user's experience, hence their willingness to provide physiological data in

different environments. Furthermore, the current system implementation incorporates low-cost sensing and processing components widely available on the market. Although the quality of these components is lower than that of medical-grade devices, it is possible to improve measurement quality by using specialized sensors and a more advanced sensor conditioning strategy. A future system prototype could be developed using superficial soldering components and miniaturized accordingly, allowing for a "plug and play" upgrade from a conventional controller. Given that the system's sensors communicate wirelessly with the VR environment, one could argue that this method could be applied to any VR controller.

7.3 Alternative Hardware Configurations

SensCon features two embedded circuits and sensors, each powered by external PowerBanks. However, we also considered other hardware configurations during the design process. Here, we discuss these alternatives and their respective benefits and drawbacks. A first option would be to integrate the battery that powers the circuits and sensors into the controller itself, increasing its robustness compared to its current configuration. In addition, the battery size restricts the maximum amount of energy supplied to the circuitry. Consequently, production versions of SensCon would require ultra-low energy consumption components. Currently, our implementation employs consumer circuits better suited for rapid prototyping rather than final production. Several software strategies for reducing power consumption can be implemented; for example, reducing the sampling rate based on the amount of activity and stopping sampling when the controller is not grasped. In its current configuration, the system continuously measures the physiological response of the participant. To allow for easier integration within the VR controller, we could reduce the component size of the circuits. With these improvements, we could explore several alternative configurations.

Embedded Circuits, External Sensors: One alternative configuration is integrating the main processing and communication circuits within the controller and attaching the sensors externally to the participant's palm or wrist. This approach enables direct measurements from the wrist or fingertips while reducing movement artifacts, but requires additional setup time that may negatively impact the user experience.

External Circuits, Surface Sensors: This alternative configuration relocates the processing and communication circuits outside the VR controller and adds superficial sensors to the grip locations, most likely in the exact locations as the current SensCon configuration. Achieving this configuration may entail designing all circuitry detachable and attachable to the VR controller. This approach enhances system versatility and flexibility for different VR controllers, but may also affect usability, grip, and robustness, depending on the attachment's ergonomics.

External Circuits, External Sensors: Similarly to the previous configuration, this alternative arrangement would position the circuitry externally to the primary body of the controller to enable it to be attached and detached. This configuration would let the sensors be positioned directly on the pulse or fingertips, as with the first configuration. This would bring the advantage of being reusable in several controllers. Still, the drawback is that it would be less robust and likely impact the usability given that the user would have to (1) set up the controller attachment and (2) setup the sensors in their hands/wrist.

7.4 Limitations and Future Work

The reported results in this study are prone to certain limitations. Here, we identify limitations and highlight space for future work and improvement for Senscon.

Evaluating Test-Retest reliability. First, our study design utilized single trials, meaning that each condition was conducted once per participant. More robust signal quality can be achieved with multiple trials. However, our conditions lasted for three minutes each, providing enough data to provide a reliable statement about the signal quality. In future work, we will first investigate how the accuracy of SensCon varies through test-retest validation.

*Effect of Controller Grip and Sensor Location.*Our study investigated the effects of sensor location on the quality of physiological signals measured during VR experiences. Specifically, we found that integrating the sensors into the VR controller provided a reliable and convenient location for measuring physiological signals, mainly when using a power grip. The power grip was the most immediate solution for our participant when asked to handle the VR controller (HTC Vive). We did not instruct participants to choose a power grip but rather that the power grip was the natural way for them to handle the VR controller, given its inherent design and affordances. While the current study focused on the power grip, future research should consider investigating other types of grips to determine how physiological signal quality may be impacted by different grip styles. Next, we will investigate how SensCon current sensor locations will perform in terms of signal quality and agreement with sensors embedded in the VR headset. Here, motion artefacts might be less observable than in finger locations. Conversely, we have to consider that acquiring an EDA signal from the head might be more influenced by thermoregulatory activity in the head rather than variation in arousal's state [81]. Similarly, PPG signal acquired from the forehead might slightly differ due to the increased vascularization and decreased vasoconstriction of scalp and brain [111].

Demographic limitations of the sample size. We need to consider some limitations in our sample related to the age range of the recruited sample. Age is a significant confounding factor in peripheral physiological signals [39]. For example, when considering the pulse transit time, which is influenced by atherosclerosis, i.e., the thickening and stiffness of blood vessel walls, which are increasing with age and can impact the accuracy of PPG measurements [84]. Furthermore, age differences can also impact physiological reactivity to a variety of arousing stimuli, e.g., affective images [32, 39] We will extend our validation to a more diverse sample considering a larger demographic diversity.

Online EDA and PPG data preprocessing. In our current implementation, we extracted physiological measures offline. To explore the feasibility and potential benefits of real-time physiological monitoring in VR adaptive settings, future work could investigate the possibility of implementing online analysis in Micropython via an on-board microcontroller or specialized ultra-low-power biometric hubs. This approach would allow real-time computation of peripheral physiological measures from the raw signal, enabling SensCon to provide immediate feedback and support real-time physiological monitoring in interactive environments. This approach would require additional hardware development, optimization, and potential trade-offs between computational complexity and power consumption. Therefore, future work should focus on exploring and evaluating the feasibility of this approach.

Generalization to real-world tasks. We chose to validate SensCon over a series of tasks representative of specific movements and cognitive processes, based on previous work [77]. These tasks were designed to be relevant to a broader community beyond just HCI and VR developers. However, further validation would benefit from a more ecological context, such as VR fitness or gaming apps, which may provide a more complex and dynamic environment to test the real-world applicability of SensCon. This would allow us to understand better how SensCon performs in scenarios that involve more erratic and everchanging movements with varied cognitive load [61] Ultimately, we

aim to design SensCon for a wide range of applications. We believe that a diverse set of validation tasks, including those focused on joint movements and various cognitive processes, is necessary to ensure that SensCon can perform well across different contexts.

Hyperscanning validation. In future work, we aim to establish embedded physiological sensing systems in hyper-scanning VR settings. Here, we will integrate SensCon into multi-user VR interactions to investigate collaborative and social VR scenarios.

8 APPLICATIONS

EDA and PPG data enable us to infer several user states, which are beneficial for interactive systems. Finally, we present use cases that benefit from SensCon as a real-time sensing system.

8.1 Sensing User Experience for Interface Assessments and Adaptations

Previous work showed that usability metrics, such as engagement [30, 49], stress [94], and workload [23, 28], are closely linked to physiological signals. Thus, real-time measurements of PPG and EDA can quantify the user experience in real-time. Virtual environments benefit from these insights as researchers and developers acquire implicit real-time feedback about their environments. SensCon integrates EDA and PPG as measures for supporting user experience designers to detect usability issues to improve them selectively. Furthermore, adaptive interfaces benefit from these usability measures by adapting the interface to either increase the user's engagement or reduce stress and workload. Physiologically aware VR environments will provide more individualized environments for the user, improving the user experience. Potential use cases include learning scenarios [80] that adapt educational material or working scenarios that provide adaptive in-situ assistance [59].

8.2 Fitness and Activity Recognition

The EDA and PPG values correspond with the physical activity of the user. Early research pointed out that increased heart rate is associated with physical activity[97]. Therefore, deriving the heart rate from SensCon enables users to estimate the activity of users in virtual environments seamlessly [103]. This information can be processed to reflect users' activity during fitness applications, i.e., balance training [31] or exergaming [79]. Additionally, virtual environments can adapt their exercises to match the physical fitness level of the user, hence optimizing the training output. Furthermore, we envision SensCon as an activity recognition sensor for virtual environments. Here, SensCon can serve as an indicator for the user's current activity, including seating, standing, or walking.

8.3 Large-Scale User Experience Assessment

Current user experience assessments are susceptible to subjective biases, lack objective real-time feedback, and require the presence of an experimenter. EDA and PPG measures can obtain objective real-time feedback for user experience assessments. However, using physiological sensing, past methods to empirically evaluate the user experience were hindered by either using a complex setup requiring prior training or large-scale data collection. SensCon overcomes these issues by facilitating the setup and data collection process by using the VR controllers only. We envision SensCon as a user-friendly tool to collect large-scale physiological data for robust user experience assessments in virtual environments.

9 CONCLUSION

This work presented SensCon, a controller-integrated physiological sensing system measuring Electrodermal Activity (EDA) and Photoplethysmography (PPG), indicating the heart rate for

Virtual Reality (VR) environments. While EDA and PPG measurements provide real-time awareness about stress, workload, and engagement to reflect on the user experience and provide environmental adaptations, such measures need medical-grade equipment requiring a laborious wearable setup. In contrast, SensCon integrates EDA and PPG sensing directly in the controller, allowing seamless ready-to-use assessments. In a user study, participants expressed a clear preference for using SensCon over medical-grade equipment. However, this comes at the cost of sensing accuracy and temporal resolution. We envision SensCon as a tool for researchers and developers to obtain a better real-time understanding of physiological ongoings when users interact with virtual environments. Through the ubiquitous embedding of EDA and PPG into VR controllers, we bridge the barriers that hinder researchers, designers, and developers from including physiological data in their systems.

10 OPEN SCIENCE

We encourage readers to reproduce and extend our results and analysis methods. Therefore our experimental setup, preprocessed datasets and analysis scripts are available on the Open Science Framework [22] (https://osf.io/h9mjs/) and on GitHub (https://github.com/mimuc/Senscon).

ACKNOWLEDGMENTS

Francesco Chiossi and Sven Mayer were supported by the Deutsche Forschungsgemeinschaft (DFG, German Research Foundation), Project-ID 251654672-TRR 161.

REFERENCES

[1] Karan Ahuja, Sven Mayer, Mayank Goel, and Chris Harrison. 2021. Pose-on-the-Go: Approximating User Pose with Smartphone Sensor Fusion and Inverse Kinematics. In *Proceedings of the 2021 CHI Conference on Human Factors in Computing Systems* (Yokohama, Japan) *(CHI '21)*. Association for Computing Machinery, New York, NY, USA, Article 9, 12 pages. https://doi.org/10.1145/3411764.3445582

[2] Karan Ahuja, Vivian Shen, Cathy Mengying Fang, Nathan Riopelle, Andy Kong, and Chris Harrison. 2022. ControllerPose: Inside-Out Body Capture with VR Controller Cameras. In *Proceedings of the 2022 CHI Conference on Human Factors in Computing Systems* (New Orleans, LA, USA) *(CHI '22)*. Association for Computing Machinery, New York, NY, USA, Article 108, 13 pages. https://doi.org/10.1145/3491102.3502105

[3] Aymen A. Alian and Kirk H. Shelley. 2014. Photoplethysmography. *Best Practice & Research Clinical Anaesthesiology* 28, 4 (2014), 395–406. https://doi.org/10.1016/j.bpa.2019.05.008

[4] Jennifer Allanson and Stephen H. Fairclough. 2004. A research agenda for physiological computing. *Interacting with computers* 16, 5 (2004), 857–878. https://doi.org/10.1016/j.intcom.2004.08.001

[5] John Allen. 2007. Photoplethysmography and its application in clinical physiological measurement. *Physiological measurement* 28, 3 (2007), R1. https://doi.org/10.1088/0967-3334/28/3/r01

[6] Douglas G Altman and J Martin Bland. 1983. Measurement in medicine: the analysis of method comparison studies. *Journal of the Royal Statistical Society: Series D (The Statistician)* 32, 3 (1983), 307–317. https://doi.org/10.2307/2987937

[7] K. Carrie Armel and Vilayanur S. Ramachandran. 2003. Projecting sensations to external objects: evidence from skin conductance response. *Proceedings of the Royal Society of London. Series B: Biological Sciences* 270, 1523 (2003), 1499–1506. https://doi.org/10.1098/rspb.2003.2364

[8] Ebrahim Babaei, Benjamin Tag, Tilman Dingler, and Eduardo Velloso. 2021. A Critique of Electrodermal Activity Practices at CHI. In *Proceedings of the 2021 CHI Conference on Human Factors in Computing Systems* (Yokohama, Japan) *(CHI '21)*. Association for Computing Machinery, New York, NY, USA, Article 177, 14 pages. https://doi.org/10.1145/3411764.3445370

[9] Anjana Bali and Amteshwar Singh Jaggi. 2015. Clinical experimental stress studies: methods and assessment. *Reviews in the Neurosciences* 26, 5 (2015), 555–579. https://doi.org/10.1515/revneuro-2015-0004

[10] Thomas Baumgartner, Lilian Valko, Michaela Esslen, and Lutz Jäncke. 2006. Neural correlate of spatial presence in an arousing and noninteractive virtual reality: an EEG and psychophysiology study. *CyberPsychology & Behavior* 9, 1 (2006), 30–45. https://doi.org/10.1089/cpb.2006.9.30

[11] Imogen H. Bell, Jennifer Nicholas, Mario Alvarez-Jimenez, Andrew Thompson, and Lucia Valmaggia. 2022. Virtual reality as a clinical tool in mental health research and practice. *Dialogues in clinical neuroscience* (2022). https://doi.org/10.31887/DCNS.2020.22.2/lvalmaggia

[12] Gershon Ben-Shakhar. 1985. Standardization within individuals: A simple method to neutralize individual differences in skin conductance. *Psychophysiology* 22, 3 (1985), 292–299.
[13] Mathias Benedek and Christian Kaernbach. 2010. Decomposition of skin conductance data by means of nonnegative deconvolution. *psychophysiology* 47, 4 (2010), 647–658. https://doi.org/10.1111/j.1469-8986.2009.00972.x
[14] Guillermo Bernal, Tao Yang, Abhinandan Jain, and Pattie Maes. 2018. PhysioHMD: A Conformable, Modular Toolkit for Collecting Physiological Data from Head-Mounted Displays. In *Proceedings of the 2018 ACM International Symposium on Wearable Computers* (Singapore, Singapore) *(ISWC '18)*. Association for Computing Machinery, New York, NY, USA, 160–167. https://doi.org/10.1145/3267242.3267268
[15] J Martin Bland and Douglas G Altman. 1999. Measuring agreement in method comparison studies. *Statistical Methods in Medical Research* 8, 2 (1999), 135–160. https://doi.org/10.1177/096228029900800204 arXiv:https://doi.org/10.1177/096228029900800204 PMID: 10501650.
[16] Andrew Garrod Bosworth. 2022. Body pose estimation using self-tracked controllers. US Patent 11,507,203.
[17] Gary Bradski and Adrian Kaehler. 2008. *Learning OpenCV: Computer vision with the OpenCV library*. O'Reilly Media, Inc., Sebastopol, California, United States.
[18] John T. Cacioppo, Gary G. Berntson, William B. Malarkey, Janice K. Kiecolt-Glaser, John F. Sheridan, Kirsten M. Poehlmann, Mary H. Burleson, John M. Ernst, Louise C. Hawkley, and Ronald Glaser. 1998. Autonomic, neuroendocrine, and immune responses to psychological stress: The reactivity hypothesis A. *Annals of the New York Academy of Sciences* 840, 1 (1998), 664–673. https://doi.org/10.1111/j.1749-6632.1998.tb09605.x
[19] John T. Cacioppo, Louis G. Tassinary, and Gary Berntson. 2007. *Handbook of psychophysiology*. Cambridge university press, Cambridge, UK. https://doi.org/10.1017/9781107415782
[20] Bryson Carrier, Brenna Barrios, Brayden D Jolley, and James W Navalta. 2020. Validity and reliability of physiological data in applied settings measured by wearable technology: A rapid systematic review. *Technologies* 8, 4 (2020), 70. https://doi.org/10.3390/technologies8040070
[21] Keyne Charlot, Jeremy Cornolo, Julien V Brugniaux, Jean-Paul Richalet, and Aurélien Pichon. 2009. Interchangeability between heart rate and photoplethysmography variabilities during sympathetic stimulations. *Physiological measurement* 30, 12 (2009), 1357. https://doi.org/10.1088/0967-3334/30/12/005
[22] Francesco Chiossi, Thomas Kosch, Luca Menghini, Steeven Villa, and Sven Mayer. 2023. SensCon: Embedding Physiological Sensing into Virtual Reality Controllers. https://doi.org/10.17605/OSF.IO/H9MJS
[23] Francesco Chiossi, Changkun Ou, and Sven Mayer. 2023. Exploring Physiological Correlates of Visual Complexity Adaptation: Insights from EDA, ECG, and EEG Data for Adaptation Evaluation in VR Adaptive Systems. In *ACM Conference on Human-Computer Interaction (CHI '23 Extended Abstracts)*. Association for Computing Machinery, Hamburg, Germany. https://doi.org/10.1145/3544549.3585624
[24] Francesco Chiossi, Yagiz Turgut, Robin Welsch, and Sven Mayer. 2023. Adapting Visual Complexity Based on Electrodermal Activity Improves Working Memory Performance in Virtual Reality. *Proc. ACM Hum.-Comput. Interact.* 7, MHCI, Article 296 (sep 2023), 26 pages. https://doi.org/10.1145/3604243
[25] Francesco Chiossi, Robin Welsch, Steeven Villa, Lewis Chuang, and Sven Mayer. 2022. Virtual Reality Adaptation Using Electrodermal Activity to Support the User Experience. *Big Data and Cognitive Computing* 6, 2 (2022), 55. https://doi.org/10.3390/bdcc6020055
[26] Francesco Chiossi, Johannes Zagermann, Jakob Karolus, Nils Rodrigues, Priscilla Balestrucci, Daniel Weiskopf, Benedikt Ehinger, Tiare Feuchtner, Harald Reiterer, Lewis L. Chuang, Marc Ernst, Andreas Bulling, Sven Mayer, and Albrecht Schmidt. 2022. Adapting visualizations and interfaces to the user. *it - Information Technology* (2022). https://doi.org/10.1515/itit-2022-0035
[27] Dongrae Cho, Jinsil Ham, Jooyoung Oh, Jeanho Park, Sayup Kim, Nak-Kyu Lee, and Boreom Lee. 2017. Detection of stress levels from biosignals measured in virtual reality environments using a kernel-based extreme learning machine. *Sensors* 17, 10 (2017), 2435. https://doi.org/10.3390/s17102435
[28] Jongyoon Choi and Ricardo Gutierrez-Osuna. 2009. Using Heart Rate Monitors to Detect Mental Stress. In *2009 Sixth International Workshop on Wearable and Implantable Body Sensor Networks*. IEEE, New York, NY, USA, 219–223. https://doi.org/10.1109/BSN.2009.13
[29] Jonny Collins, Holger Regenbrecht, Tobias Langlotz, Yekta Said Can, Cem Ersoy, and Russell Butson. 2019. Measuring Cognitive Load and Insight: A Methodology Exemplified in a Virtual Reality Learning Context. In *2019 IEEE International Symposium on Mixed and Augmented Reality (ISMAR '19)*. IEEE, New York, NY, USA, 351–362. https://doi.org/10.1109/ISMAR.2019.00033
[30] Elena Di Lascio, Shkurta Gashi, and Silvia Santini. 2018. Unobtrusive Assessment of Students' Emotional Engagement during Lectures Using Electrodermal Activity Sensors. *Proc. ACM Interact. Mob. Wearable Ubiquitous Technol.* 2, 3, Article 103 (sep 2018), 21 pages. https://doi.org/10.1145/3264913
[31] Dennis Dietz, Carl Oechsner, Changkun Ou, Francesco Chiossi, Fabio Sarto, Sven Mayer, and Andreas Butz. 2022. Walk This Beam: Impact of Different Balance Assistance Strategies and Height Exposure on Performance and Physiological

Arousal in VR. In *28th ACM Symposium on Virtual Reality Software and Technology* (Tsukuba, Japan) *(VRST '22)*. Association for Computing Machinery, New York, NY, USA, Article 32, 12 pages. https://doi.org/10.1145/3562939.3567818

[32] Sigrun Doberenz, Walton T Roth, Eileen Wollburg, Nina I Maslowski, and Sunyoung Kim. 2011. Methodological considerations in ambulatory skin conductance monitoring. *International Journal of Psychophysiology* 80, 2 (2011), 87–95. https://doi.org/10.1016/j.ijpsycho.2011.02.002

[33] Nurettin Özgür Doğan. 2018. Bland-Altman analysis: A paradigm to understand correlation and agreement. *Turkish journal of emergency medicine* 18, 4 (2018), 139–141. https://doi.org/10.1016/j.tjem.2018.09.001

[34] Henrik H. Ehrsson, Katja Wiech, Nikolaus Weiskopf, Raymond J. Dolan, and Richard E. Passingham. 2007. Threatening a rubber hand that you feel is yours elicits a cortical anxiety response. *Proceedings of the National Academy of Sciences* 104, 23 (2007), 9828–9833. https://doi.org/10.1073/pnas.0610011104

[35] Sergio Estupiñán, Francisco Rebelo, Paulo Noriega, Carlos Ferreira, and Emília Duarte. 2014. Can virtual reality increase emotional responses (Arousal and Valence)? A pilot study. In *Design, User Experience, and Usability. User Experience Design for Diverse Interaction Platforms and Environments: Third International Conference, DUXU 2014, Held as Part of HCI International 2014, Heraklion, Crete, Greece, June 22-27, 2014, Proceedings, Part II 3*. Springer, Cham, Switzerland, 541–549. https://doi.org/10.1007/978-3-319-07626-3_51

[36] Anne M Euser, Friedo W Dekker, and Saskia Le Cessie. 2008. A practical approach to Bland-Altman plots and variation coefficients for log transformed variables. *Journal of clinical epidemiology* 61, 10 (2008), 978–982. https://doi.org/10.1016/j.jclinepi.2007.11.003

[37] Society for Psychophysiological Research Ad Hoc Committee on Electrodermal Measures, Wolfram Boucsein, Don C. Fowles, Sverre Grimnes, Gershon Ben-Shakhar, Walton T. Roth, Michael E. Dawson, and Diane L. Filion. 2012. Publication Recommendations for Electrodermal Measurements. *Psychophysiology* 49, 8 (2012), 1017–1034. https://doi.org/10.1111/j.1469-8986.1981.tb03024.x

[38] Jonathan Freeman, Steve E. Avons, Don E. Pearson, and Wijnand A. IJsselsteijn. 1999. Effects of sensory information and prior experience on direct subjective ratings of presence. *Presence* 8, 1 (1999), 1–13. https://doi.org/10.1162/105474699566017

[39] Joachim Gavazzeni, Stefan Wiens, and Håkan Fischer. 2008. Age effects to negative arousal differ for self-report and electrodermal activity. *Psychophysiology* 45, 1 (2008), 148–151. https://doi.org/10.1111/j.1469-8986.2007.00596.x

[40] Alireza Mazloumi Gavgani, Keith V Nesbitt, Karen L Blackmore, and Eugene Nalivaiko. 2017. Profiling subjective symptoms and autonomic changes associated with cybersickness. *Autonomic Neuroscience* 203 (2017), 41–50. https://doi.org/10.1016/j.autneu.2016.12.004

[41] Davide Giavarina. 2015. Understanding bland altman analysis. *Biochemia medica* 25, 2 (2015), 141–151. https://hrcak.srce.hr/139769

[42] Grace E. Giles, Caroline R. Mahoney, Tad T. Brunyé, Holly A. Taylor, and Robin B. Kanarek. 2014. Stress effects on mood, HPA axis, and autonomic response: comparison of three psychosocial stress paradigms. *PloS one* 9, 12 (2014), e113618. https://doi.org/10.1371/journal.pone.0113618

[43] Gyeong-Nam Gimhae. 2013. Six human factors to acceptability of wearable computers. *International Journal of Multimedia and Ubiquitous Engineering* 8, 3 (2013), 103–114. http://www.sersc.org/journals/IJMUE/vol8_no3_2013/10.pdf

[44] Francesco Giordana, Veselin Efremov, Gael Sourimant, Silvia Rasheva, Natasha Tatarchuk, and Callum James. 2018. Virtual Production in 'Book of the Dead': Technicolor's Genesis Platform, Powered by Unity. In *ACM SIGGRAPH 2018 Real-Time Live!* Association for Computing Machinery, New York, NY, USA. https://doi.org/10.1145/3229227.3229235

[45] Stefan Gradl, Markus Wirth, Nico Mächtlinger, Romina Poguntke, Andrea Wonner, Nicolas Rohleder, and Bjoern M. Eskofier. 2019. The Stroop Room: A Virtual Reality-Enhanced Stroop Test. In *25th ACM Symposium on Virtual Reality Software and Technology* (Parramatta, NSW, Australia) *(VRST '19)*. Association for Computing Machinery, New York, NY, USA, Article 28, 12 pages. https://doi.org/10.1145/3359996.3364247

[46] Klaus Gramann, Ryan Mckendrick, Carryl Baldwin, Raphaëlle Roy, Camille Jeunet, Ranjana Mehta, and Giovanni Vecchiato. 2021. Grand field challenges for cognitive neuroergonomics in the coming decade. *Frontiers in Neuroergonomics* 2 (2021). https://doi.org/10.3389/fnrgo.2021.643969

[47] Catharina C. Grant, Dina C. J. van Rensburg, Nina Strydom, and Margaretha Viljoen. 2011. Importance of tachogram length and period of recording during noninvasive investigation of the autonomic nervous system. *Annals of Noninvasive Electrocardiology* 16, 2 (2011), 131–139. https://doi.org/10.1111/j.1542-474X.2011.00422.x

[48] Simone Grassini and Karin Laumann. 2020. Questionnaire measures and physiological correlates of presence: A systematic review. *Frontiers in psychology* 11 (2020), 349. https://doi.org/10.3389/fpsyg.2020.00349

[49] Mariam Hassib, Stefan Schneegass, Philipp Eiglsperger, Niels Henze, Albrecht Schmidt, and Florian Alt. 2017. EngageMeter: A System for Implicit Audience Engagement Sensing Using Electroencephalography. In *Proceedings of the 2017 CHI Conference on Human Factors in Computing Systems* (Denver, Colorado, USA) *(CHI '17)*. Association for

Computing Machinery, New York, NY, USA, 5114–5119. https://doi.org/10.1145/3025453.3025669

[50] Mandy X. Hu, Femke Lamers, Eco J. C. de Geus, and Brenda WJH Penninx. 2016. Differential Autonomic Nervous System Reactivity in Depression and Anxiety During Stress Depending on Type of Stressor. *Psychosomatic medicine* 78, 5 (2016), 562–572. https://doi.org/10.1097/PSY.0000000000000313

[51] Wen Huang, Rod D Roscoe, Mina C Johnson-Glenberg, and Scotty D Craig. 2021. Motivation, engagement, and performance across multiple virtual reality sessions and levels of immersion. *Journal of Computer Assisted Learning* 37, 3 (2021), 745–758. https://doi.org/10.1111/jcal.12520

[52] Yi-Jheng Huang, Kang-Yi Liu, Suiang-Shyan Lee, and I-Cheng Yeh. 2021. Evaluation of a hybrid of hand gesture and controller inputs in virtual reality. *International Journal of Human–Computer Interaction* 37, 2 (2021), 169–180. https://doi.org/10.1080/10447318.2020.1809248

[53] Weiwei Jiang, Kangning Yang, Maximiliane Windl, Francesco Chiossi, Benjamin Tag, Sven Mayer, and Zhanna Sarsenbayeva. 2022. Current Challenges of Using Wearable Devices for Online Emotion Sensing. *arXiv preprint arXiv:2208.05206* (2022). https://doi.org/10.48550/arXiv.2208.05206

[54] Cornelia Kappeler-Setz, Franz Gravenhorst, Johannes Schumm, Bert Arnrich, and Gerhard Tröster. 2013. Towards long term monitoring of electrodermal activity in daily life. *Personal and ubiquitous computing* 17, 2 (2013), 261–271. https://doi.org/10.1007/s00779-011-0463-4

[55] Armağan Karahanoğlu and Çiğdem Erbuğ. 2011. Perceived Qualities of Smart Wearables: Determinants of User Acceptance. In *Proceedings of the 2011 Conference on Designing Pleasurable Products and Interfaces* (Milano, Italy) *(DPPI '11)*. Association for Computing Machinery, New York, NY, USA, Article 26, 8 pages. https://doi.org/10.1145/2347504.2347533

[56] Ladislav Karrach, Elena Pivarčiová, and Pavol Božek. 2020. Identification of QR code perspective distortion based on edge directions and edge projections analysis. *Journal of imaging* 6, 7 (2020), 67. https://doi.org/10.3390/jimaging6070067

[57] Kwanguk Kim, M Zachary Rosenthal, David Zielinski, and Rachel Brady. 2012. Comparison of desktop, head mounted display, and six wall fully immersive systems using a stressful task. In *2012 IEEE Virtual Reality Workshops (VRW)*. IEEE, New York, NY, USA, 143–144. https://doi.org/10.1109/VR.2012.6180922

[58] Jocelyne Kiss, Geoffrey Edwards, Ernesto Morales, Sherezada Ochoa, Bruno Bernier, et al. 2019. Enhancing Mobile VR Immersion: A Multimodal System of Neural Networks Approach to an IMU Gesture Controller. *Electronic Imaging* 2019, 2 (2019), 184–1. https://doi.org/10.2352/ISSN.2470-1173.2019.2.ERVR-184

[59] Thomas Kosch, Markus Funk, Albrecht Schmidt, and Lewis L. Chuang. 2018. Identifying Cognitive Assistance with Mobile Electroencephalography: A Case Study with In-Situ Projections for Manual Assembly. *Proc. ACM Hum.-Comput. Interact.* 2, EICS, Article 11 (jun 2018), 20 pages. https://doi.org/10.1145/3229093

[60] Thomas Kosch, Jakob Karolus, Havy Ha, and Albrecht Schmidt. 2019. Your Skin Resists: Exploring Electrodermal Activity As Workload Indicator During Manual Assembly. In *Proceedings of the ACM SIGCHI Symposium on Engineering Interactive Computing Systems* (Valencia, Spain) *(EICS '19)*. ACM, New York, NY, USA, Article 8, 5 pages. https://doi.org/10.1145/3319499.3328230

[61] Thomas Kosch, Jakob Karolus, Johannes Zagermann, Harald Reiterer, Albrecht Schmidt, and Pawel Wozniak. 2023. A Survey on Measuring Cognitive Workload in Human-Computer Interaction. *Comput. Surveys*, Article 1 (jan 2023), 37 pages. https://doi.org/10.1145/3582272

[62] George Alex Koulieris, Kaan Akşit, Michael Stengel, Rafał K Mantiuk, Katerina Mania, and Christian Richardt. 2019. Near-eye display and tracking technologies for virtual and augmented reality. In *Computer Graphics Forum*, Vol. 38. Wiley Online Library, Hoboken, New Jersey, USA, 493–519. https://doi.org/10.1111/cgf.13654

[63] Peter J Lang, Mark K Greenwald, Margaret M Bradley, and Alfons O Hamm. 1993. Looking at pictures: Affective, facial, visceral, and behavioral reactions. *Psychophysiology* 30, 3 (1993), 261–273. https://doi.org/10.1111/j.1469-8986.1993.tb03352.x

[64] László Laufer and Bottyán Németh. 2008. Predicting User Action from Skin Conductance. In *Proceedings of the 13th International Conference on Intelligent User Interfaces* (Gran Canaria, Spain) *(IUI '08)*. Association for Computing Machinery, New York, NY, USA, 357–360. https://doi.org/10.1145/1378773.1378829

[65] Huy Viet Le, Sven Mayer, Katrin Wolf, and Niels Henze. 2016. Finger Placement and Hand Grasp during Smartphone Interaction. In *Proceedings of the 2016 CHI Conference Extended Abstracts on Human Factors in Computing Systems* (San Jose, California, USA) *(CHI EA '16)*. Association for Computing Machinery, New York, NY, USA, 2576–2584. https://doi.org/10.1145/2851581.2892462

[66] James R Lewis. 2018. The system usability scale: past, present, and future. *International Journal of Human–Computer Interaction* 34, 7 (2018), 577–590. https://doi.org/10.1080/10447318.2018.1455307

[67] Yue Li, Lu Zheng, and Xuewen Wang. 2019. Flexible and wearable healthcare sensors for visual reality health-monitoring. *Virtual Reality & Intelligent Hardware* 1, 4 (2019), 411–427. https://doi.org/10.1016/j.vrih.2019.08.001

[68] Wan-Hua Lin, Dan Wu, Chunyue Li, Heye Zhang, and Yuan-Ting Zhang. 2014. Comparison of heart rate variability from PPG with that from ECG. In *The international conference on health informatics*. Springer, Cham, Switzerland, 213–215. https://doi.org/10.1007/978-3-319-03005-0_54

[69] Tiffany Luong, Ferran Argelaguet, Nicolas Martin, and Anatole Lécuyer. 2020. Introducing mental workload assessment for the design of virtual reality training scenarios. In *2020 IEEE Conference on Virtual Reality and 3D User Interfaces (VR)*. IEEE, New York, NY, USA, 662–671. https://doi.org/10.1109/VR46266.2020.00089

[70] Tiffany Luong, Nicolas Martin, Anais Raison, Ferran Argelaguet, Jean-Marc Diverrez, and Anatole Lécuyer. 2020. Towards real-time recognition of users mental workload using integrated physiological sensors into a VR HMD. In *2020 IEEE International Symposium on Mixed and Augmented Reality (ISMAR)*. IEEE, New York, NY, USA, 425–437. https://doi.org/10.1109/ISMAR50242.2020.00068

[71] David T Lykken and Peter H Venables. 1971. Direct measurement of skin conductance: A proposal for standardization. *Psychophysiology* 8, 5 (1971), 656–672. https://doi.org/10.1111/j.1469-8986.1971.tb00501.x

[72] Dominique Makowski, Tam Pham, Zen J. Lau, Jan C. Brammer, François Lespinasse, Hung Pham, Christopher Schölzel, and SH Chen. 2021. NeuroKit2: A Python toolbox for neurophysiological signal processing. *Behavior research methods* 53, 4 (2021), 1689–1696. https://doi.org/10.3758/s13428-020-01516-y

[73] Srinivas Mantha, Michael F Roizen, Lee A Fleisher, Ronald Thisted, and Joseph Foss. 2000. Comparing methods of clinical measurement: reporting standards for Bland and Altman analysis. *Anesthesia & Analgesia* 90, 3 (2000), 593–602. https://doi.org/10.1097/00000539-200003000-00018

[74] Javier Marín-Morales, Carmen Llinares, Jaime Guixeres, and Mariano Alcañiz. 2020. Emotion recognition in immersive virtual reality: From statistics to affective computing. *Sensors* 20, 18 (2020), 5163. https://doi.org/10.3390/s20185163

[75] Michael Meehan, Brent Insko, Mary Whitton, and Frederick P. Brooks. 2002. Physiological Measures of Presence in Stressful Virtual Environments. *ACM Trans. Graph.* 21, 3 (jul 2002), 645–652. https://doi.org/10.1145/566654.566630

[76] Luca Menghini, Nicola Cellini, Aimee Goldstone, Fiona C Baker, and Massimiliano de Zambotti. 2020. A standardized framework for testing the performance of sleep-tracking technology: step-by-step guidelines and open-source code. *Sleep* 44, 2 (10 2020). https://doi.org/10.1093/sleep/zsaa170 arXiv:https://academic.oup.com/sleep/article-pdf/44/2/zsaa170/36244924/zsaa170.pdf zsaa170.

[77] Luca Menghini, Evelyn Gianfranchi, Nicola Cellini, Elisabetta Patron, Mariaelena Tagliabue, and Michela Sarlo. 2019. Stressing the accuracy: Wrist-worn wearable sensor validation over different conditions. *Psychophysiology* 56, 11 (2019), e13441. https://doi.org/10.1111/psyp.13441

[78] Nir Milstein and Ilanit Gordon. 2020. Validating measures of electrodermal activity and heart rate variability derived from the empatica e4 utilized in research settings that involve interactive dyadic states. *Frontiers in Behavioral Neuroscience* (2020), 148. https://doi.org/10.3389/fnbeh.2020.00148

[79] John E. Muñoz, M. Cameirão, S. Bermúdez i Badia, and E. Rubio Gouveia. 2018. Closing the Loop in Exergaming - Health Benefits of Biocybernetic Adaptation in Senior Adults. In *Proceedings of the 2018 Annual Symposium on Computer-Human Interaction in Play* (Melbourne, VIC, Australia) *(CHI PLAY '18)*. Association for Computing Machinery, New York, NY, USA, 329–339. https://doi.org/10.1145/3242671.3242673

[80] Zhigeng Pan, Adrian David Cheok, Hongwei Yang, Jiejie Zhu, and Jiaoying Shi. 2006. Virtual reality and mixed reality for virtual learning environments. *Computers & Graphics* 30, 1 (2006), 20–28. https://doi.org/10.1016/j.cag.2005.10.004

[81] Andrew F. H. Payne, Anne M. Schell, and Michael E. Dawson. 2016. Lapses in skin conductance responding across anatomical sites: Comparison of fingers, feet, forehead, and wrist. *Psychophysiology* 53, 7 (2016), 1084–1092. https://doi.org/10.1111/psyp.12643

[82] Riccardo Pernice, Michal Javorka, Jana Krohova, Barbora Czippelova, Zuzana Turianikova, Alessandro Busacca, and Luca Faes. 2018. Reliability of short-term heart rate variability indexes assessed through photoplethysmography. In *2018 40th Annual International Conference of the IEEE Engineering in Medicine and Biology Society (EMBC'18)*. IEEE, New York, NY, USA, 5610–5513. https://doi.org/10.1109/EMBC.2018.8513634

[83] Livia Petrescu, Cătălin Petrescu, Oana Mitruț, Gabriela Moise, Alin Moldoveanu, Florica Moldoveanu, and Marius Leordeanu. 2020. Integrating biosignals measurement in virtual reality environments for anxiety detection. *Sensors* 20, 24 (2020), 7088. https://doi.org/10.3390/s20247088

[84] C.C.Y. Poon and Y.T. Zhang. 2005. Cuff-less and Noninvasive Measurements of Arterial Blood Pressure by Pulse Transit Time. In *2005 IEEE Engineering in Medicine and Biology 27th Annual Conference*. IEEE, New York, NY, USA, 5877–5880. https://doi.org/10.1109/IEMBS.2005.1615827

[85] Hugo F Posada-Quintero and Jeffrey B Bolkhovsky. 2019. Machine learning models for the identification of cognitive tasks using autonomic reactions from heart rate variability and electrodermal activity. *Behavioral Sciences* 9, 4 (2019), 45. https://doi.org/10.3390/bs9040045

[86] Alan Poston. 2000. Human engineering design data digest. *Washington, DC: Department of Defense Human Factors Engineering Technical Advisory Group* (2000), 61–75.

[87] Ramesh Kumar Ramakrishnan, Rahul Gavas, Venkata Subramaninan Viraraghavan, Lalit Kumar Hissaria, Arpan Pal, and P. Balamuralidhar. 2020. Monitoring The Early Physiological Effects of Fitness Regimes Using PPG Signals. In *2020 IEEE International Conference on Pervasive Computing and Communications Workshops (PerCom Workshops)*. IEEE, New York, NY, USA, 1–5. https://doi.org/10.1109/PerComWorkshops48775.2020.9156258

[88] Ian M. Raugh, Hannah C. Chapman, Lisa A. Bartolomeo, Cristina Gonzalez, and Gregory P. Strauss. 2019. A comprehensive review of psychophysiological applications for ecological momentary assessment in psychiatric populations. *Psychological assessment* 31, 3 (2019), 304. https://doi.org/10.1037/pas0000651

[89] Giuseppe Riva, Fabrizia Mantovani, Claret Samantha Capideville, Alessandra Preziosa, Francesca Morganti, Daniela Villani, Andrea Gaggioli, Cristina Botella, and Mariano Alcañiz. 2007. Affective interactions using virtual reality: the link between presence and emotions. *Cyberpsychology & behavior* 10, 1 (2007), 45–56. https://doi.org/10.1089/cpb.2006.9993

[90] Justas Šalkevicius, Robertas Damaševičius, Rytis Maskeliunas, and Ilona Laukienė. 2019. Anxiety level recognition for virtual reality therapy system using physiological signals. *Electronics* 8, 9 (2019), 1039. https://doi.org/10.3390/electronics8091039

[91] Axel Schäfer and Jan Vagedes. 2013. How accurate is pulse rate variability as an estimate of heart rate variability?: A review on studies comparing photoplethysmographic technology with an electrocardiogram. *International journal of cardiology* 166, 1 (2013), 15–29. https://doi.org/10.1016/j.ijcard.2012.03.119

[92] Valentin Schwind, Pascal Knierim, Nico Haas, and Niels Henze. 2019. Using Presence Questionnaires in Virtual Reality. In *Proceedings of the 2019 CHI Conference on Human Factors in Computing Systems* (Glasgow, Scotland Uk) *(CHI '19)*. Association for Computing Machinery, New York, NY, USA, 1–12. https://doi.org/10.1145/3290605.3300590

[93] Nandakumar Selvaraj, Ashok Jaryal, Jayashree Santhosh, Kishore K. Deepak, and Sneh Anand. 2008. Assessment of heart rate variability derived from finger-tip photoplethysmography as compared to electrocardiography. *Journal of medical engineering & technology* 32, 6 (2008), 479–484. https://doi.org/10.1080/03091900701781317

[94] Cornelia Setz, Bert Arnrich, Johannes Schumm, Roberto La Marca, Gerhard Tröster, and Ulrike Ehlert. 2010. Discriminating Stress From Cognitive Load Using a Wearable EDA Device. *IEEE Transactions on Information Technology in Biomedicine* 14, 2 (2010), 410–417. https://doi.org/10.1109/TITB.2009.2036164

[95] Mel Slater. 2004. How colorful was your day? Why questionnaires cannot assess presence in virtual environments. *Presence* 13, 4 (2004), 484–493. https://doi.org/10.1162/1054746041944849

[96] Mel Slater. 2018. Immersion and the illusion of presence in virtual reality. *British journal of psychology* 109, 3 (2018), 431–433. https://doi.org/10.1111/bjop.12305

[97] Phyllis K Stein, Ali A Ehsani, Peter P Domitrovich, Robert E Kleiger, and Jeffrey N Rottman. 1999. Effect of exercise training on heart rate variability in healthy older adults. *American heart journal* 138, 3 (1999), 567–576. https://doi.org/10.1007/s00421-009-1089-3

[98] Paul Streli, Rayan Armani, Yi Fei Cheng, and Christian Holz. 2023. HOOV: Hand Out-Of-View Tracking for Proprioceptive Interaction Using Inertial Sensing. In *Proceedings of the 2023 CHI Conference on Human Factors in Computing Systems* (Hamburg, Germany) *(CHI '23)*. Association for Computing Machinery, New York, NY, USA, Article 310, 16 pages. https://doi.org/10.1145/3544548.3581468

[99] Erin Treacy Solovey, Daniel Afergan, Evan M. Peck, Samuel W. Hincks, and Robert J. K. Jacob. 2015. Designing Implicit Interfaces for Physiological Computing: Guidelines and Lessons Learned Using FNIRS. *ACM Trans. Comput.-Hum. Interact.* 21, 6, Article 35 (jan 2015), 27 pages. https://doi.org/10.1145/2687926

[100] Marieke van Dooren, Joris H Janssen, et al. 2012. Emotional sweating across the body: Comparing 16 different skin conductance measurement locations. *Physiology & behavior* 106, 2 (2012), 298–304. https://doi.org/10.1016/j.physbeh.2012.01.020

[101] Sjoerd van Halem, Eeske Van Roekel, Lara Kroencke, Niclas Kuper, and Jaap Denissen. 2020. Moments that matter? On the complexity of using triggers based on skin conductance to sample arousing events within an experience sampling framework. *European Journal of Personality* 34, 5 (2020), 794–807. https://doi.org/10.1002/per.2252

[102] Don van Ravenzwaaij, Rei Monden, Jorge N Tendeiro, and John Ioannidis. 2019. Bayes factors for superiority, non-inferiority, and equivalence designs. *BMC medical research methodology* 19, 1 (2019), 1–12. https://doi.org/10.1186/s12874-019-0699-7

[103] José Varela-Aldás, Esteban M Fuentes, Guillermo Palacios-Navarro, and Iván García-Magariño. 2019. A comparison of heart rate in normal physical activity vs. immersive virtual reality exergames. In *International Conference on Human Systems Engineering and Design: Future Trends and Applications*. Springer, Cham, Switzerland, 684–689. https://doi.org/10.1007/978-3-030-27928-8_104

[104] Viswanath Venkatesh, Michael G. Morris, Gordon B. Davis, and Fred D. Davis. 2003. User acceptance of information technology: Toward a unified view. *MIS quarterly* (2003), 425–478. https://doi.org/10.2307/30036540

[105] Roger Vilardaga, Jonathan B. Bricker, and Michael G. McDonell. 2014. The promise of mobile technologies and single case designs for the study of individuals in their natural environment. *Journal of Contextual Behavioral Science* 3, 2

(2014), 148–153. https://doi.org/10.1016/j.jcbs.2014.03.003

[106] Francesco Walker, Debargha Dey, Marieke Martens, Bastian Pfleging, Berry Eggen, and Jacques Terken. 2019. Feeling-of-Safety Slider: Measuring Pedestrian Willingness to Cross Roads in Field Interactions with Vehicles. In *Extended Abstracts of the 2019 CHI Conference on Human Factors in Computing Systems* (Glasgow, Scotland Uk) *(CHI EA '19)*. Association for Computing Machinery, New York, NY, USA, 1–6. https://doi.org/10.1145/3290607.3312880

[107] Michael Wilkinson, Zachary H. Pugh, Aaron Crowson, Jing Feng, Christopher B. Mayhorn, and Douglas J. Gillan. 2019. Seeing in slow motion: manipulating arousal in virtual reality. In *Proceedings of the Human Factors and Ergonomics Society Annual Meeting*, Vol. 63. SAGE Publications Sage CA, Los Angeles, CA, 1649–1653. https://doi.org/10.1177/1071181319631512

[108] Mark G. Williams, Andrew Mathews, and Colin MacLeod. 1996. The emotional Stroop task and psychopathology. *Psychological bulletin* 120, 1 (1996), 3. https://doi.org/10.1037/0033-2909.120.1.3

[109] Jacob O. Wobbrock, Leah Findlater, Darren Gergle, and James J. Higgins. 2011. The Aligned Rank Transform for Nonparametric Factorial Analyses Using Only Anova Procedures. In *Proceedings of the SIGCHI Conference on Human Factors in Computing Systems* (Vancouver, BC, Canada) *(CHI '11)*. Association for Computing Machinery, New York, NY, USA, 143–146. https://doi.org/10.1145/1978942.1978963

[110] Ruiyang Yin, Depeng Wang, Shufang Zhao, Zheng Lou, and Guozhen Shen. 2021. Wearable sensors-enabled human–machine interaction systems: from design to application. *Advanced Functional Materials* 31, 11 (2021), 2008936. https://doi.org/10.1002/adfm.202008936

[111] Tomas Ysehak Abay, Kamran Shafqat, and Panayiotis A Kyriacou. 2019. Perfusion changes at the forehead measured by photoplethysmography during a head-down tilt protocol. *Biosensors* 9, 2 (2019), 71. https://doi.org/10.3390/bios9020071

[112] Clint Zeagler. 2017. Where to Wear It: Functional, Technical, and Social Considerations in on-Body Location for Wearable Technology 20 Years of Designing for Wearability. In *Proceedings of the 2017 ACM International Symposium on Wearable Computers* (Maui, Hawaii) *(ISWC '17)*. Association for Computing Machinery, New York, NY, USA, 150–157. https://doi.org/10.1145/3123021.3123042

[113] Yang Zhang, Wolf Kienzle, Yanjun Ma, Shiu S. Ng, Hrvoje Benko, and Chris Harrison. 2019. ActiTouch: Robust Touch Detection for On-Skin AR/VR Interfaces. In *Proceedings of the 32nd Annual ACM Symposium on User Interface Software and Technology* (New Orleans, LA, USA) *(UIST '19)*. Association for Computing Machinery, New York, NY, USA, 1151–1159. https://doi.org/10.1145/3332165.3347869

A APPENDIX

Table 4. Table of the computed correlations across the computed dependent variables. MG stands for Medical-Grade device. HR = heart rate; SCL = Skin Conductance Level; nsSCRs = average frequency of the detected nonspecific skin conductance responses

	MG - HR	SensCon - HR	MG - SCL	SensCon - SCL	MG - nsSCRs Peaks
SensCon - HR	.541	–	–	–	–
MG - SCL	.141	.0985	–	–	–
SensCon - SCL	.137	.004	.139	–	–
MG - nsSCRs Peaks	−.275	−.045	−.119	−.326	–
SensCon - nsSCRs Peaks	.209	.03	.175	.077	−.262

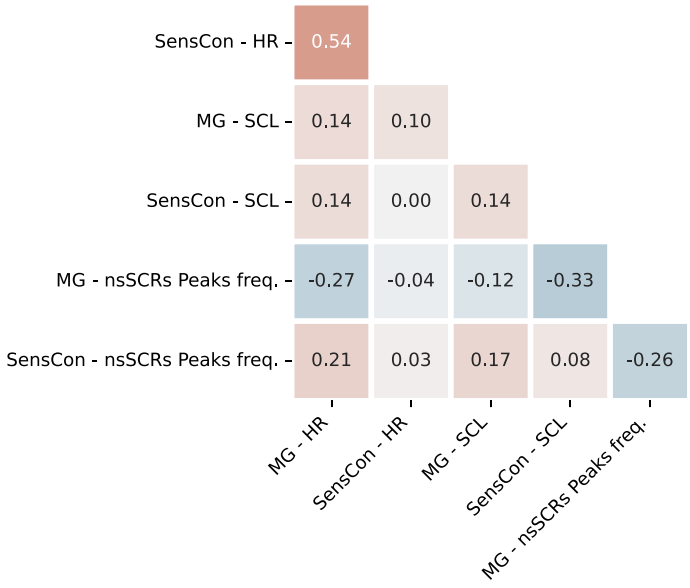

Fig. 15. *Correlation Matrix.* Colors indicate the strength of Pearson correlation coefficients. HR = heart rate; SCL = Skin Conductance Level; nsSCRs = average frequency of the detected nonspecific skin conductance responses. MG suffix represents the Medical-Grade device.

Received January 2023; revised May 2023; accepted June 2023

Table 5. Physiological signals and Bland-Altman statistics across the six tasks. **HR** Heart rate; **SCL**, Skin conductance level; **nsSCRs**, non-specific skin conductance responses; **SD**, standard deviation; **CI**, confidence intervals (computed using parametric bootstrap with 10,000 replicates); **LOA**, limit of agreement; cases requiring log-transformation prior to data analysis. When a proportional bias was detected, a linear model of discrepancies as a function mean measures was specified, and 95% CI were reported for the model intercept (b0) and slope (b1). When heteroscedasticity was detected, a linear model of the absolute residuals as a function of mean measures was specified, and 95% CI were reported for the model's intercept (c0) and slope (c1).

	Condition	SensCon		Reference		Bias	Lower LOA	Upper LOA
		M	SD	M	SD	M (SD) [95% CI]	[95% CI]	[95% CI]
HR (bpm)	Seating	91.7	10.79	91.98	15.41	-0.28 (11.98) [-7.44, 6.6]	-23.76 [-30.86, -16.84]	23.19 [15.96, 29.81]
	Standing	98.18	7.03	98.38	15.74	-.2 (14.09) [-7.65, 8.69]	-27.81 [-35.23, -18.53]	27.41 [20.16, 36.21]
	Walking	98.59	8.12	100.54	18.29	-1.95 (16.06) [-10.59, 7.99]	-33.42 [-42.21, -23.46]	29.52 [20.77, 39.87]
	Selection	94.65	8.12	97.47	14.65	-2.82 (15.05) [-10.49, 6.93]	B - M × .29 [.18, .46]	B + M × .29 [.18, .46]
	N-back	93.14	18.28	98.05	16.70	-4.9 (12.58) [-12.06, 2.34]	B - 2.46 × (33.09 - .24 × M) c0 = [29.43, 82.07], c1 = [-.75, -.2]	B + 2.46 × (33.09 - .24 × M) c0 = [29.43, 82.07], c1 = [-.75, -.2]
	Stroop	92.98	13.54	100.54	16.49	-7.56 (13.63) [-15.58, .49]	-34.27 [-42.35, -26.26]	19.15 [11.28, 27.13]
SCL (standardized units)	Seating	−.12	.26	.01	.05	-.04 + 1.68 × M b0 = [-.09, .03], b1 = [1.47, 2.03]	B - .17 [.1, .31]	B + .17 [.1, .31]
	Standing	.04	.3	.02	.05	-.04 + 1.83 × M b0 = [-.1, .04], b1 = [1.49, 2.12]	B - .18 [.14, .32]	B + .18 [.14, .32]
	Walking	−.05	.23	.07	.15	-.12 (.25) [-.27, .03]	B - 2.46 × (.17 + .43 × M) c0 = [.13, .2], c1 = [.17, 1.58]	B + 2.46 × (.17 + .43 × M) c0 = [.13, .2], c1 = [.17, 1.58]
	Selection	.09	.26	.04	.06	-.05 + 1.57 × M b0 = [-.11, .01], b1 = [.65, 3.23]	B - .20 [.13, .36]	B + .20 [.13, .36]
	N-back	−.12	.25	−.02	.08	.00 + 1.5 × M b0 = [-.08, .1], b1 = [.79, 2.26]	B - 2.46 × (.10 - .23 × M) c0 = [.05, .12], c1 = [-.85, -.05]	B + 2.46 × (.10 - .23 × M) c0 = [.05, .12], c1 = [-.85, -.05]
	Stroop	.07	.15	−.01	.06	.02 + 1.88 × M b0 = [-.05, .08], b1 = [.85, 3.03]	B - .25 [.16, .42]	B + .25 [.16, .42]
nsSCRs (peaks/min)	Seating	.06	.03	.08	.07	.09 - 1.56 × M b0 = [.02, .25], b1 = [-5.1, -.97]	B - .12 [.08, .21]	B + .12 [.08, .21]
	Standing	.06	.03	.06	.05	.08 - 1.23 × M b0 = [-.02, .23], b1 = [-4.16, -0.11]	B - 2.46 × (.02 + .49 × M) c0 = [-.06, .04], c1 = [0.1, 1.79]	B + 2.46 × (.02 + .49 × M) c0 = [-.06, .04], c1 = [.1, 1.79]
	Walking	.05	.03	.09	.07	.11 - 2.1 × M b0 = [-.02, .29], b1 = [-5.55, -.4]	B - .13 [.1, .21]	B + .13 [.1, .21]
	Selection	.04	.01	.06	.04	.08 - 1.93 × M b0 = [.03, .14], b1 = [-3.86, -1.26]	B - .06 [.04, .09]	B + .06 [.04, .09]
	N-back	.07	.04	.05	.04	.01 (.05) [-.02, .04]	B - 2.46 × (-.02 + .98 × M) c0 = [-.13, -.02], c1 = [1, 2.85]	B + 2.46 × (-.02 + .98 × M) c0 = [-.13, -.02], c1 = [1, 2.85]
	Stroop	0.08	.04	0.07	.06	0.01 (0.08) [-0.03, 0.06]	B - M × 1.36 [1.08, 2.06]	B + M × 1.36 [1.08, 2.06]